The Potential of Sodium Sulfur Battery Energy Storage to Enable Further Integration of Wind

A THESIS
SUBMITTED TO THE FACULTY OF THE GRADUATE SCHOOL
OF THE UNIVERSITY OF MINNESOTA
BY

Saurabh Tewari

IN PARTIAL FULFILLMENT OF THE REQUIREMENTS
FOR THE DEGREE OF
MASTER OF SCIENCE

Advisor: Prof. Ned Mohan

February, 2012

Acknowledgements

First and foremost, I thank my advisor Prof. Ned Mohan for giving me the opportunity to work on this project, and the guidance towards completing it to satisfaction. Prof. Mohan's interest and enthusiasm for the topic has been extremely helpful and motivating over the course of this work. I would also acknowledge his contribution towards developing the Wind Energy Essentials course that served to develop my understanding of the subject matter significantly.

I thank Prof. Charles Geyer for his help towards an important part of this thesis, as a co-author of one of the publications from the presented research, as the instructor for Theory of Statistics I, and for agreeing to be in the examining committee.

I thank Prof. Bruce Wollenberg in his capacity as the chair of the examining committee and as the instructor for the Power Systems course. Even though I served as a T.A. and had taken similar classes in past, I learned significantly from his teaching.

This project was conceived and funded in part by Xcel Energy, and gratitude is due to Xcel for providing the necessary framework, data, and financial support. The cooperation from numerous individuals at Xcel, most notably James B. Himelic was critical to the success of this project. An important amount of data for the presented analyses was provided by the Midwest Independent Transmission System Operator, Inc. (MISO) and the National Renewable Energy Labs (NREL). Their willingness to freely distribute their data towards advancing research is wholeheartedly appreciated. Special thanks go to Rao Konidena at MISO for his insight and discussions. Additional financial support from the Initiative for Renewable Energy and the Environment (IREE), University of Minnesota, is gratefully acknowledged.

Finally I owe it to my research group and to my peers for their help, suggestions and insight, and for creating a friendly atmosphere facilitating research.

Dedication

To my parents, sisters, and teachers.

Abstract

Wind generation is a strong contender towards securing clean, renewable and reliable energy supply. Seamless integration of higher amounts of wind generation into the existing power system requires flexibility and accurate forecasts. Coupling energy storage with wind generation has the potential of improving the on-peak availability of wind, and mitigating the natural variability and the forecast errors in wind. Further, energy storage can check the curtailment of wind under low load conditions. Under the liberalized markets, the effects of additional wind on the system manifest themselves in the energy and operating reserve prices. Offering storage in these markets has the potential to stabilize the prices while earning revenue to justify the investment in storage. This thesis presents analyses of the value of storage towards improving the on-peak availability of wind generation, smoothing the wind farm output, and compensating for the forecast errors. The forecast errors from Persistence forecast are examined on a local and aggregated basis, and a statistical model for the local wind power forecast error has been developed. A strategy for optimizing the revenue in the energy markets has been proposed, and an analysis of the value offered by storage in the operating reserve market is presented. A strategy for siting the storage at the financially optimal location has also been proposed.

Contents

List of Tables

List of Figures

Chapter 1

Introduction

Securing reliable electricity supply with minimal impact on the environment necessitates the use of clean and renewable sources of electricity. Wind generation is a strong contender towards meeting a major share of our electricity needs in the future. Among renewables, the current contribution of electricity produced by wind is exceeded only by hydro, and wind is growing at a rate faster than any other renewable source of energy [1]; there is a strong commitment towards increasing the proportion of wind generation at all levels of government, nationally and internationally [2–4].

Wind differs fundamentally from the traditional fossil fuel based generation in its variability and limited predictability. Several studies have examined the feasibility, costs, and impacts of higher penetration of wind on the existing system, and it has been established that that it is indeed possible to source 20% or more of our electricity needs from wind. However, to meet these ambitious targets, it is imperative to have accurate forecasts and flexibility in the power system [4–10]: good forecasts enable economically efficient planning of generation to meet the expected load; of course, the generation mix must be flexible enough to accommodate the forecasted wind. In addition, there should be some flexibility to compensate for the forecast errors and short-term variations in the wind generation.

Even in the absence of wind, flexible generation is necessary to meet the time varying demand, the errors in the load forecast, and unexpected events like outages. The existing power system has means of meeting these requirements using different kinds of generators that comprise the intermediate generation, peaking generation, and the

operating reserves (regulating, spinning and standing) [11]. Addition of wind generation merely imposes more on these aforementioned means of handling unexpected events and variability. Therefore, traditional generation has the potential to accommodate more wind without resorting to options like energy storage or demand response. However, using fossil fuel based generation to meet the requirements imposed by wind has certain disadvantages that can be eliminated by using energy storage or demand response:

1. Avoided fuel costs and pollution from the fast acting peaking generation [11].

2. Use of rigid but efficient units to serve the baseload [11], while avoiding baseload bottoming and wind curtailment [12].

3. Eliminating rotor fatigue associated with generators providing compensation for faster variations [13, 14].

In addition to eliminating the disadvantages mentioned above, storage and demand response can enhance the on-peak availability of wind generation by either time shifting the load (demand response) or by time shifting the wind generated energy (using energy storage). Shifting wind generation is equivalent to leveling the load from the perspective of rest of the generation that has several advantages e.g. deferring or avoiding capacity and transmission upgrade, reduced transmission and distribution (T&D) losses and more robust system stability [15–17].

Radical developments in the last two decades have seen the emergence of Regional Transmission Organizations (RTOs), Transmission System Operators (TSOs), or Independent System Operators (ISOs) that operate energy and ancillary services markets worldwide [18–23]. Although wind generation receives a generally favorable treatment in many of these markets [24], the rules governing the participation of wind are no longer as lax as they were a few years ago: according to the 2009 version of [24], wind generation was exempt from penalties imposed on deviations from the schedules under Midwest ISO, which is not the case anymore in 2011. Forecasting plays an important role in scheduling wind generation and in the assessment of these penalties [24–26]; and therefore, as Market Participants (MPs), it is necessary for the wind generators to understand the errors associated with wind forecasts and the effect of these errors on the revenue earned by the wind resource. Energy storage coupled to a wind farm can also

serve as a solution towards mitigating the penalties associated with departures from the schedules, in addition to the benefits discussed earlier.

The energy and operating reserve prices in the modern markets are a product of supply and demand of energy and reserves, and vary with time and physical location [27]:

- The locational marginal price (LMP) of energy is the cost of meeting incremental demand at a location at that time, under the generation and transmission constraints at that location.

- Under normal operating conditions (sufficient energy available) the market clearing price (MCP), used in the context of reserves, is determined by the cost of supplying enough reserves, as deemed necessary by the ISO. Under the scarce energy conditions, the prices for the reserves are capped at the value of lost load (VOLL).

In the light of above, it could be expected that the additional reserve requirements and the energy excess/deficit imposed by a higher amount of wind generation would manifest themselves in the LMPs and MCPs. The effect of reserve availability and system reliability on the value of reserves has been researched in [28] and [29]; viewed in conjunction with the research on reserve requirements in the high wind penetration scenarios reported in [8,9], it can be concluded that more wind generation would imply generally higher prices for operating reserves. Energy storage could be used to provide operating reserves, thereby mitigating the prices of reserves.

The effect of higher wind penetration on the LMPs has been reported in [30], and it is shown that under transmission constraints, the variability in the LMPs tends to increase with higher penetration of wind on the system. Excess or deficit wind generation can easily destabilize the LMPs in absence of enough transmission capability. Energy storage has the potential to stabilize the prices by absorbing excess generation and compensating for deficit generation. Further, the financially optimal location for siting storage would also be the best choice from a transmission system point of view because the locational variability of the LMPs is a result of transmission constraints [11].

Therefore, energy storage would aid the integration of wind even when added to the system from a purely financial perspective.

1.1 The Sodium Sulfur (NAS) battery at Luverne, MN

Xcel Energy, a major U.S. utility, installed a 1 MW, 7.2 MWh Sodium Sulfur battery in Luverne, MN in 2008 towards its 'Wind to Battery' project [31]. The purpose of this project was to evaluate the ability of Sodium Sulfur (NAS) battery energy storage (referred to as battery hereafter) to aid the integration of wind generation. This battery was manufactured by NGK Insulators Ltd., Japan. The battery is located near a 11.55 MW wind farm owned by Minwind Energy LLC.

1.1.1 Operating principle

The battery operates on the principle of a reversible redox reaction between sodium and sulfur. The operating temperature is 300°C and the electrodes are molten during operation. The electrolyte is solid β-alumina. [32]

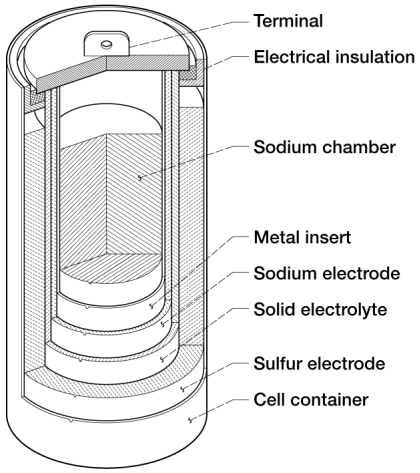

Figure 1.1: Cutaway illustration of the battery. Image courtesy NASA

The redox reaction governing the operation of the battery is (1.1)

$$2\,\mathrm{Na} + x\,\mathrm{S} \underset{\text{charging}}{\overset{\text{disch.}}{\rightleftharpoons}} \mathrm{Na_2S}_x \tag{1.1}$$

1.1.2 Features and applications

According to NGK's catalog [32], some of the prominent features of the battery are:

- 3 to 5 times the energy density of lead acid batteries.
- High pulse power capability and prompt response.
- Long calendar and cycle life: 15 years and 4500 cycles for a 90% depth-of-discharge (DOD).
- 85% round trip DC efficiency.

The major application areas are load leveling, peak shaving and power quality. Another example of a utility scale NAS battery installation is the 100 kW, 720 kWh battery in Ohio installed for peak shaving and power quality applications [33].

1.2 Brief overview of Midwest ISO markets

The Midwest Independent Transmission System Operator, Inc. (MISO) [18] operates energy and operating reserve markets in 12 U.S. states and the Canadian province of Manitoba. Energy demand and reserve requirement are cleared in the forward and spot markets, known as the Day Ahead (DA) Energy and Operating Reserve Market and Real Time (RT) Energy and Operating Reserve Market. The energy prices corresponding to these markets are known as Day Ahead Locational Marginal Price (DALMP) and Real Time Locational Marginal Price (RTLMP). A location for which the DALMP and RTLMP are calculated is called an Elemental Pricing Node (EPNode). A Commercial Pricing Node (CPNode) consists of one or more EPNodes: the LMPs, and the Market Clearing Prices (MCP) paid to the operating reserves, are published at every CPNode.

The DA market is cleared one day in advance of the operating day and hourly prices and schedules are posted based on the load forecast, generation offers and demand bids, and reserve offers and reserve requirements. The RT market is cleared every 5 minutes during the operating day using a similar process, and prices vary between different 5 minute intervals. However, hourly average of the prices is used for settlement. The markets are cleared on the principle of Security Constrained Unit Commitment (SCUC) and Security Constrained Economic Dispatch (SCED).

Bulk of the energy is settled in the DA markets or through bilateral agreements between the Market Participants (MPs). However, the DA schedules are based on load forecasts. The imbalances due to forecast errors and other unforeseen events are settled in the RT market. The instantaneous balancing of generation and load is handled by regulation reserves. The details of market clearing and settlement can be found in [27, 34].

Although market settlement is an involved process that takes into account a number of charges and credits [34], simplifying assumptions have been made for the presented analyses:

- The energy in DA markets is bought and sold at DALMP with no additional charge or credit.
- The energy in RT markets is bought and sold at RTLMP with no additional charge or credit. The intra-hour movement in the RTLMP is ignored because the data is not accessible publicly.
- Participation is considered only in the DA operating reserve market. The battery is paid the SERREGMCP[1], and no additional charges or credits are considered.

1.3 Scope and organization of this thesis

This thesis presents analyses evaluating the value and the ability of the battery towards the following tasks:

- Shifting wind generation to enhance the on-peak availability of wind in context of the Minwind wind farm (basic generation shifting).
- Smoothing the minute-to-minute variations in the energy generated by the Minwind wind farm (ramp rate limiting).
- Value of the battery in the MISO energy markets when dispatched according to the economic dispatch strategy developed by Xcel Energy, and optimal location for siting the battery (Economic dispatch and location analysis).

[1]Stored Energy Resource Regulation Market Clearing Price

- Value of the battery in the MISO operating reserve markets.

In addition to above, the following items are presented pertaining to wind and energy storage in general:

- A statistical model for the wind power forecast error from short-term Persistence forecasts has been developed and applied to calculate the penalties for uninstructed deviations in the MISO RT markets. The value of energy storage towards mitigating these penalties has been analyzed.
- The net forecast error over a large area has been examined, and it is shown that the distribution of the net error tends towards a Normal distribution with much lower spread than the error from individual wind farms.
- A strategy to dispatch energy storage exclusively in the RT market has been proposed.

All analyses are carried out in the context of MISO markets. The thesis is organized as follows:

1. Chapter 1: Introduction.
2. Chapter 2 presents the analysis of the ability and the value of the battery to shift wind generation to on-peak (basic generation shifting).
3. Chapter 3 presents the analysis of the battery to mitigate the ramp rate of the wind farm output, and integration of generation shifting with this objective (ramp rate limiting, ramp rate limiting with basic generation shifting).
4. Chapter 4 examines the forecast errors from Persistence forecast on a local and aggregated basis, and develops a statistical model for the local error. The model is then used to evaluate the value of energy storage towards mitigating the penalties for uninstructed deviations in the MISO RT markets for forecast based scheduling.
5. Chapter 5 describes a strategy to dispatch the battery in the MISO RT markets, and optimizes the parameters of the resource and the resource offer.

6. Chapter 6 describes the strategy developed by Xcel Energy to dispatch the battery in the DA and RT markets and uses this strategy to identify the financially optimal locations to site the battery.

7. Chapter 7 analyzes the value of the battery in the MISO operating reserve markets.

8. Chapter 8 summarizes the analyses and concludes the thesis.

Chapter 2

Basic generation shifting

This chapter evaluates the ability and the value of the battery to shift wind generation from off-peak to on-peak. The generation data is from the Minwind wind farm, the prices data is from MISO, and the load data is from NSP[1]. The off-peak and on-peak intervals are determined using the load on NSP. The analysis is performed in three stages:

1. It is first shown that the battery is successfully able to shift energy, wind generated or otherwise, from off-peak to on-peak. Actual charging/discharging data from the field is used. (wind-grid charging)

2. With confidence in the battery's ability to shift the generation, the battery operation is simulated using long term data (1 year). The battery is allowed to charge only from wind generation (wind only charging). The wind generation time series is multiplied by suitable scaling factors to simulate 11.55 MW, 10 MW, 5 MW, 2.5 MW, and 1 MW installed wind scenarios for the same 1 MW, 7.2 MWh battery. For each of these cases, the histograms of the daily maximum SOC (state of charge) are plotted.

3. The value from shifting wind generation is evaluated for all the cases, followed by a discussion on the optimal storage to wind ratio.

[1]Xcel Energy's territory under the MISO footprint is known as NSP, named after Northern States Power.

Fig. 2.1 shows the monthly demand on NSP for the year 2009 and Table 2.1 tabulates the hours arranged in the order of decreasing demand for each month.

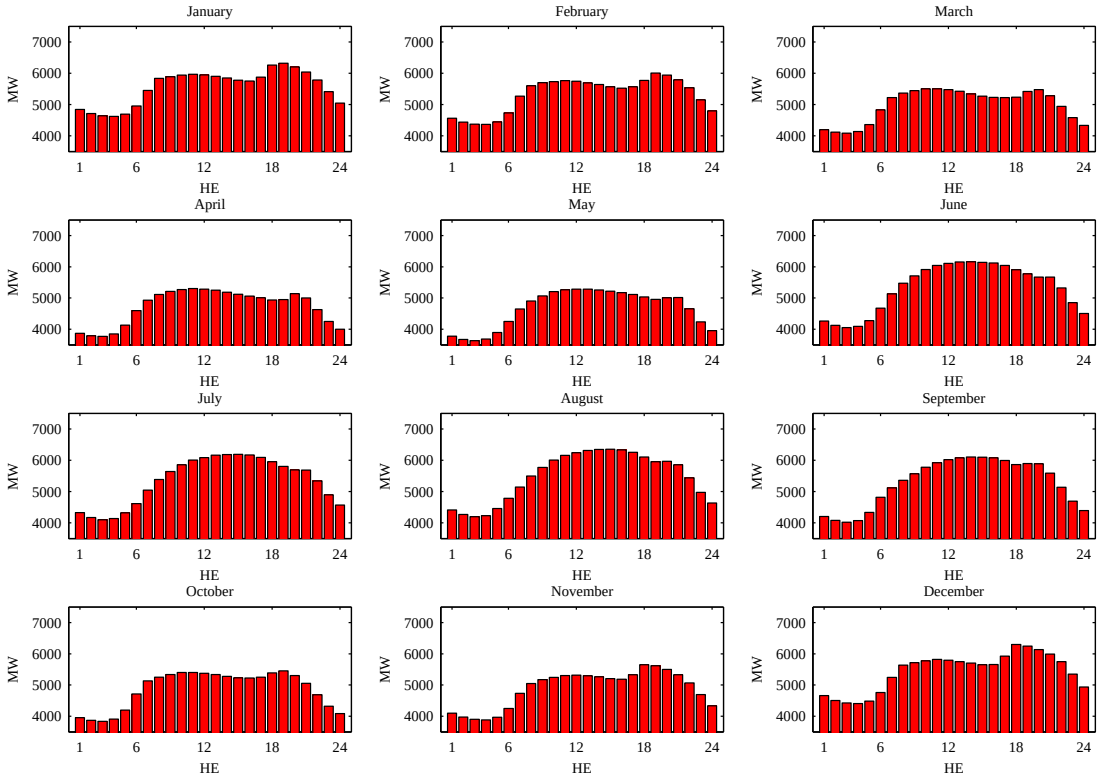

Figure 2.1: NSP load for different months (Year 2009).

For each day, 8 hours form the designated charging period (off-peak) and 6 hours form the designated discharging period (on-peak). These hours are chosen on the basis of average monthly load from Table 2.1.

Jan	Feb	Mar	Apr	May	Jun	Jul	Aug	Sep	Oct	Nov	Dec
19	19	10	11	12	14	15	15	14	19	18	18
18	20	11	12	13	13	14	14	15	11	19	19
20	21	12	10	11	15	16	16	16	10	20	20
21	18	20	13	14	16	13	13	13	18	17	21
11	11	9	9	15	12	17	17	12	12	21	17
12	12	13	14	10	11	12	12	17	13	12	11
10	10	19	20	16	17	11	11	11	9	11	12
13	9	8	15	17	10	18	18	19	20	13	10
9	13	14	8	9	18	10	10	20	14	14	22
17	14	21	16	18	19	19	20	18	17	10	13
14	8	15	17	21	9	20	19	10	8	15	9
8	15	18	21	20	20	21	21	21	15	16	14
22	17	16	19	19	21	9	9	9	16	9	16
15	22	7	18	8	8	8	8	8	7	22	15
16	16	17	7	22	22	22	22	22	21	8	8
7	7	22	22	7	7	7	7	7	6	7	23
23	23	6	6	6	23	23	23	6	22	23	7
24	24	23	23	23	6	6	6	23	23	24	24
6	6	5	5	24	24	24	24	24	5	6	6
1	1	24	24	5	5	1	5	5	24	1	1
2	5	1	1	1	1	5	1	1	1	2	2
5	2	4	4	4	2	2	2	2	4	5	5
3	3	2	2	2	4	4	4	4	2	3	3
4	4	3	3	3	3	3	3	3	3	4	4

Table 2.1: Hours arranged in the order of decreasing demand (Year 2009).

2.1 Wind-grid charging

The purpose of this testing was to validate that the battery can be brought to a 100% SOC with grid support, without exception, to effectively shift the generation, wind or otherwise. Data for this mode was collected for the week starting May 18, 2011 and ending May 24, 2011.

The designated charging and discharging hours were chosen based on the historical demand on NSP for the year 2009. The specified designated charging hours were HE22, HE23, HE24, HE01, HE02, HE03, HE04; and HE05 if needed. The specified designated discharging hours were HE11, HE12, HE10, HE13, HE14, HE09, HE15 (in this priority).

The results from this mode are plotted in Fig. 2.2. The designated charging hours are an hour ahead of the specifications because of daylight savings. The designated discharging hours differ because of the way the DESS (Distributed Energy Storage System) works under this mode — the discharge period needs to be centered at the hour of maximum demand.

Even though there is some offset between the specified and actual periods, the conclusions are not affected:

- The battery SOC is successfully brought to 100% before the beginning of every discharge period.
- The battery is able to shift generation from off-peak to on-peak.

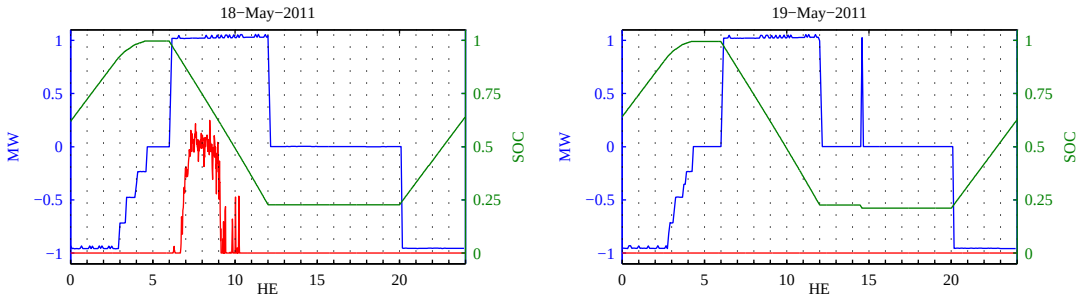

(a) (b)

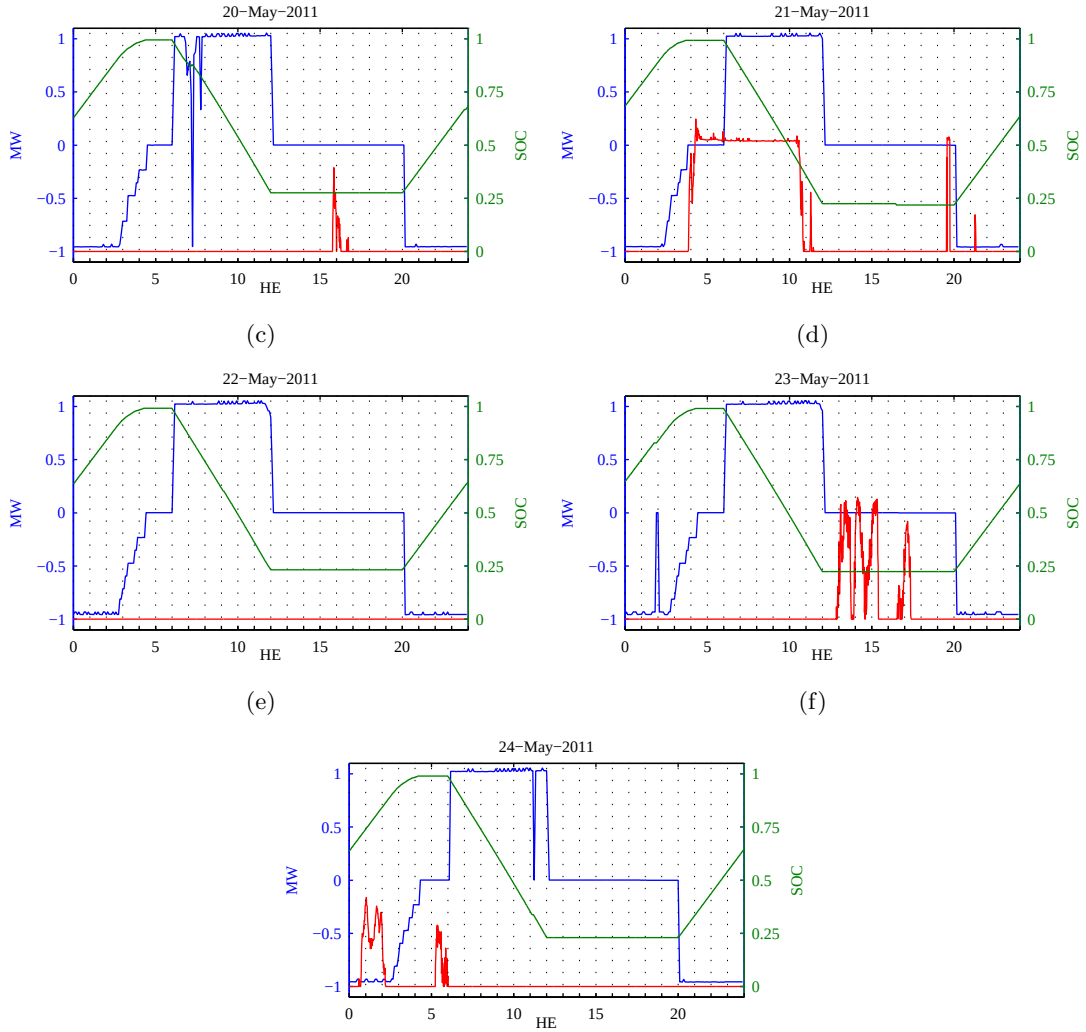

Figure 2.2: Wind-grid charging: The green plot is the SOC, the blue plot is the power supplied by the battery (−ve sign implies charging), and the red plot is the power available to the battery from wind generation only (saturated at 1 MW for clarity). In most cases, enough wind generation is available to charge the battery. How often does the wind generation fall short is investigated next.

2.2 Wind only charging

In this section the ability of battery to shift the *wind only* generation from off-peak to on-peak is evaluated. The simulation is carried out at different values of the scaling factor to effectively vary the ratio of storage to wind generation.

Using real charging/discharging data for this mode was not feasible because of the time needed for testing; however, as evidenced from Fig. 2.2, the battery characteristics are near ideal since it can operate at its rated power (± 1 MW) for extended periods of time. Following parameters and data were used:

1. 1 MW, 7.2 MWh battery with ideal charging characteristics: the battery can be charged at its rated power continuously.

2. DC efficiency = 85% [32]

3. Wind generation data for the year 2007 from the 11.55 MW Minwind wind farm. The power generation time series was multiplied by 1, 10/11.55, 5/11.55, 2.5/11.55 and 1/11.55 to simulate wind farm rating ranging from 11.55 MW down to 1 MW for the same 1 MW battery. Data was available for 360 days.

4. 8 designated charging hours and 6 designated discharging hours for each different month were chosen from Table 2.1.

5. Day Ahead (DA) and Real Time (RT) Locational Marginal Prices (LMPs) for MINN.HUB of Midwest ISO (MISO) for the year 2009.

Although the wind generation data was available for the year 2007, it is treated as though it was from the year 2009. This is not an issue because the wind patterns change over a much slower time scale.

The battery losses were assumed to be geometrically distributed between charging and discharging. Therefore for every MWh drawn from the wind farm, the stored energy was simulated to increase by $\sqrt{0.85}$ MWh while for every MWh supplied, the stored energy was simulated to decrease by $1/\sqrt{0.85}$ MWh, resulting in a net efficiency of 85%. The minimum SOC was set to $\sim$10%. Under the assumption made about distributing losses and this setting for minimum SOC, the battery would be able to discharge for about 6 hours during on-peak.

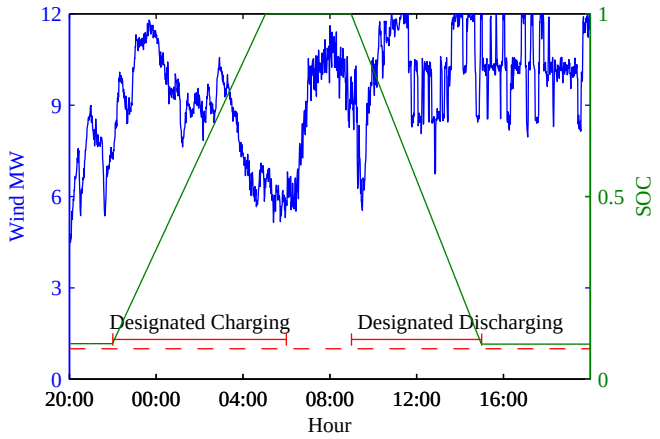

Figure 2.3: Simulated charging and discharging for wind only scenario

Fig. 2.3 shows the simulated charging/discharging for a day in May 2009. The bold blue plot is the wind generation, the bold green plot is the SOC and the dashed red line is generation = 1 MW. The designated charging period begins at 2200 hours and ends at 0600 hours. The designated discharging period begins at 0900 hours and ends at 1500 hours.

It is seen that the battery charges at full power up to 100% SOC and discharges down to $\sim$ 10% SOC at the end of designated discharging period of 6 hours.

The charging was simulated for different scaling factors and the maximum SOC for each day was recorded. The distribution of maximum SOC attained for different scaling factors is plotted in Fig. 2.4.

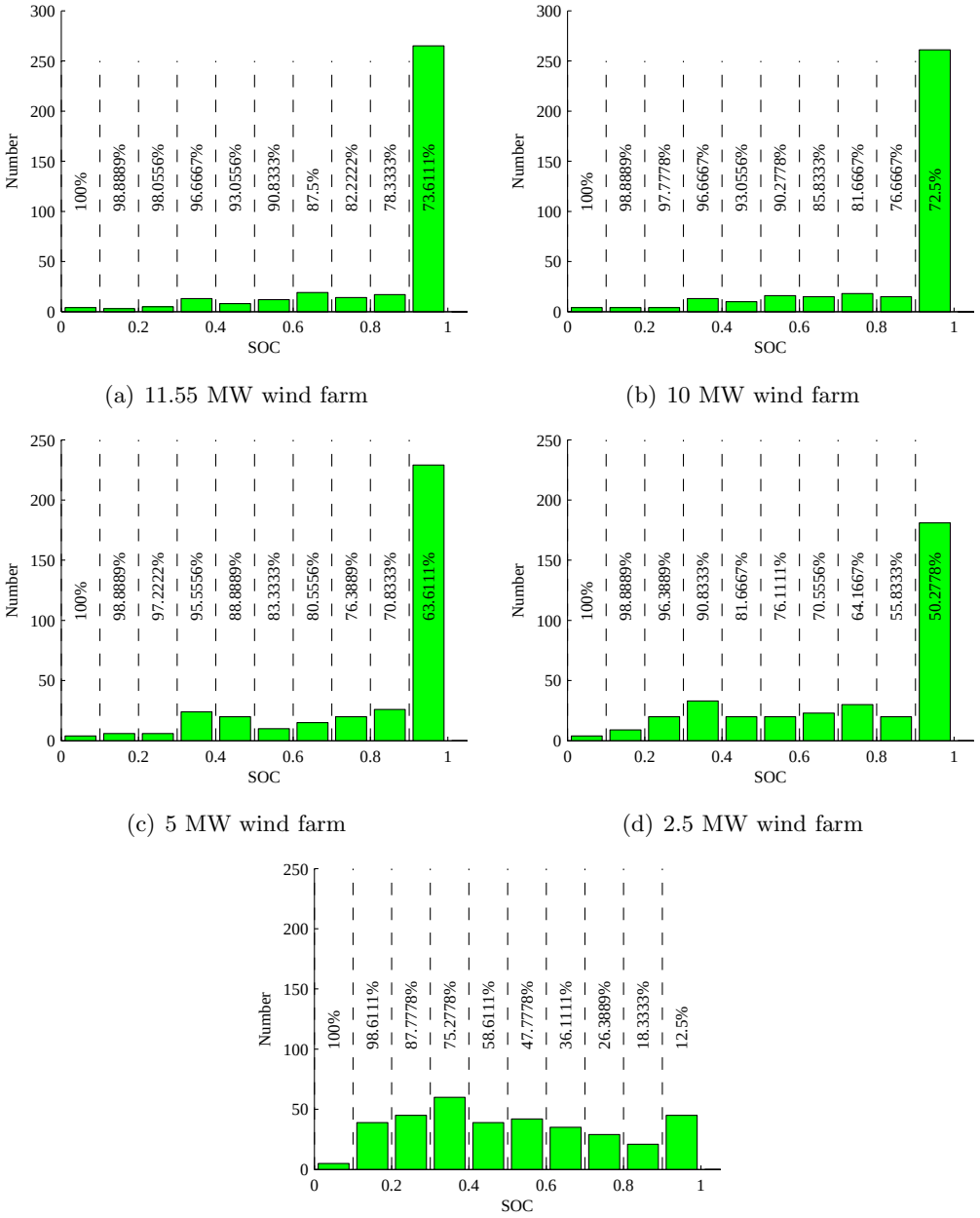

(a) 11.55 MW wind farm

(b) 10 MW wind farm

(c) 5 MW wind farm

(d) 2.5 MW wind farm

(e) 1 MW wind farm

Figure 2.4: Distribution of maximum SOC attained for wind only charging. The effective rating of the wind farm after scaling is mentioned under each subfigure. The numbers right of the dashed lines are the % exceedances at dashed lines.

2.2.1 Optimal ratio of storage to wind

If it is desired that the storage be able to supply during 6 hours of highest load everyday, and the battery parameters like efficiency and maximum depth of discharge (DOD) are fixed, then the MWh to MW ratio of the storage gets fixed. In the case of this battery, this ratio is 7.2 MWh per MW. For this ratio, 85% efficiency and 90% DOD, the battery would be able to serve 6 peak load hours.

With the MWh/MW of battery fixed, the optimal ratio of storage to wind is essentially the inverse of installed wind per MW storage. In this analysis this ratio (storage/wind) is varied from 1/11.55, up to 1/1. It is intuitively clear that the optimal ratio would depend upon the value in generation shifting, that can be broken into:

- Revenue from discharging the battery at peak load. The electricity prices tend to follow the load and it is reasonable to expect that prices would be higher at peak load.
- Savings from avoiding costlier peaking generation.
- Inherent value in making wind generation available on-peak:
  - Avoided greenhouse emissions from fossil fuel based peaking generators and carbon credits.
  - Maximization of the wind generation value by mitigating the scenarios in which wind generators need to curtail their output in event of low load.
  - Qualification (of wind generators) as a reliable system resource with guaranteed on-peak availability and capacity value.
- Inherent value of storage: storage installed primarily to enable guaranteed on-peak availability of wind generation can be used as a system resource with, but not limited to, the following secondary benefits:
  - Up/Down regulation capability (please see chapter 7).
  - Limiting the ramp rate of wind generation (please see section 3.4).

It is relatively straight forward to attach a $ amount to some of the value propositions above (e.g. transactions in the energy market) while some are not so easily characterized

in terms of dollars (e.g. environmental benefits). For the purpose of this work, the $ amounts for the following value propositions have been considered:

- Transactions in the energy market.
- Avoided cost of peaking generation.
- Value in letting wind generators operate during low load, quantified in terms of the Production Tax Credit (PTC).

The value from other applications of storage is evaluated in other sections of this report.

Procedure

For this analysis, the battery is offered as a 1 MW load in the MISO DA markets for the 8 hour designated charging period and as a generator for the 6 hour designated discharging period.

- The Asset Owner (AO) pays the DALMP for the charging period and receives the DALMP for the discharging period.
- It is possible that the battery attains 100% SOC before the end of the charging period in which case the energy bought in the DA market is sold at the RTLMP. In an event of battery not being at 100% SOC at the beginning of discharging period, the energy committed in the DA market is bought from the RT market (true up). Since this mode allows the storage to charge *only* from wind, in an event when enough wind energy is not available to charge the storage at its maximum rate (1 MW), the AO still pays the DALMP but receives the RTLMP multiplied by the MWs the wind generation falls short of 1 MW.
- Further, for every MWh generated that goes towards charging the battery, the total value of generation shifting is increased by the Production Tax Credit (PTC) for wind; the value of PTC available from EIA [35] is 19 $/MWh in 2003 dollars that is adjusted to 22.23 $/MWh in 2009 dollars using an inflation rate of 1.17 from the Bureau of Labor Statistics [36].

- Finally, it is assumed that the peak generation is served by Combustion turbines is absence of stored energy. Therefore, savings corresponding to the difference between the levelized cost of wind generation (48 $/MWh) and Combustion turbines based generation (70 $/MWh) are added for every MWh of peak load served. The data for the levelized cost of generation available from [35] in 2003 dollars and is adjusted for inflation in accordance with [36]. However, the cost of wind generation is assumed without crediting the Production Tax Credits. If the PTC is included, the levelized cost of wind generation would come down to 29 $/MWh.

Define the following:

MWh_WIND	Energy generated by wind during designated charging period
DA_VOL	Volume cleared in DA market
E_WIND	Energy supplied by wind generation, to the battery
E_PEAK	Energy served by storage at peak load
RT_VOL	Adjustments made in RT market
$\text{E\_PEAK}_{\max}$	Maximum possible energy that could be served by storage on-peak
PTC	Production Tax Credits in 2003 dollars [35]
c_WIND	Levelized cost of wind generation in 2003 dollars [35]
c_COMB	Levelized cost of Combustion turbine generation in 2003 dollars [35]
$k_{2003,2009}$	Inflation rate [36]

Some of the quantities above are taken from the cited sources while others are calculated as

$$\text{DA\_VOL} = \begin{cases} -1 & \text{during designated charging period} \\ +1 & \text{during designated discharging period} \end{cases}$$

$$\text{E\_WIND} = \begin{cases} \min(\text{MWh\_WIND}, 1) & \text{during designated charging period if SOC} < 1 \\ 0 & \text{otherwise} \end{cases}$$

$$\text{E\_PEAK} = \begin{cases} 1 & \text{during designated discharging period if SOC} > 0.1 \\ 0 & \text{otherwise} \end{cases}$$

With the definitions above, the RT_VOL can be written as

$$\text{RT\_VOL} = \begin{cases} -\text{DA\_VOL} - \text{E\_WIND} & \text{during designated charging period} \\ -\text{DA\_VOL} + \text{E\_PEAK} & \text{during designated discharging period} \\ 0 & \text{otherwise} \end{cases}$$

The maximum possible energy that could be served at peak load ($\text{E\_PEAK}_{\max}$) is simply 6 MWh energy for every operating day.

The revenue from the perspective of the battery AO can therefore be written as

$$\begin{aligned} \text{REVENUE} = \sum_{\text{day}=1}^{360} \sum_{\text{hour}=1}^{24} & \text{DA\_VOL}_{\text{day,hour}} \times \text{DA\_LMP}_{\text{day,hour}} \\ & + \text{RT\_VOL}_{\text{day,hour}} \times \text{RT\_LMP}_{\text{day,hour}} \\ & + k_{2003,2009} \times \text{E\_WIND}_{\text{day,hour}} \times \text{PTC} \end{aligned} \tag{2.1}$$

The additional savings on the system level by avoiding costlier generation would be

$$\text{SAVINGS} = \sum_{\text{day}=1}^{360} \sum_{\text{hour}=1}^{24} (\text{c\_COMB} - \text{c\_WIND}) \times \text{E\_PEAK}_{\text{day,hour}} \times k_{2003,2009} \tag{2.2}$$

And the total value of generation shifting quantified in this analysis would be the sum of revenue and savings from (2.1) and (2.2). Other quantities of interest are: the ratio of generation shifted — the ratio of energy served on-peak against the total wind generation off-peak; the ratio of storage utilized — the ratio of energy served on-peak against the maximum possible energy that could have been served on-peak; and the ratio of revenue against energy served on-peak.

For every MWh served on-peak, the battery incurs loss in its lifetime and in that sense the ratio of revenue against energy served on-peak could be a measure of the return on investment (ROI). The listed quantities can be defined as

$$\begin{aligned} \text{Ratio shifted} &= \frac{\text{E\_PEAK}}{\text{MWh\_WIND}} \\ \text{Storage utilized} &= \frac{\text{E\_PEAK}}{\text{E\_PEAK}_{\max}} \\ \$/\text{MWh served} &= \frac{\text{REVENUE} + \text{SAVINGS}}{\text{E\_PEAK}} \end{aligned}$$

Results

Fig. 2.5 shows the positive and negative contributions to the value of generation shifting. Positive contributions are from selling the stored energy in DA market during designated discharging, selling excess energy during designated charging in the RT market, PTC, and additional savings realized by avoiding costlier generation.

Negative contributions are from buying the energy to charge the battery in DA market during designated charging, and from having to buy energy during designated discharging in event of deficient SOC.

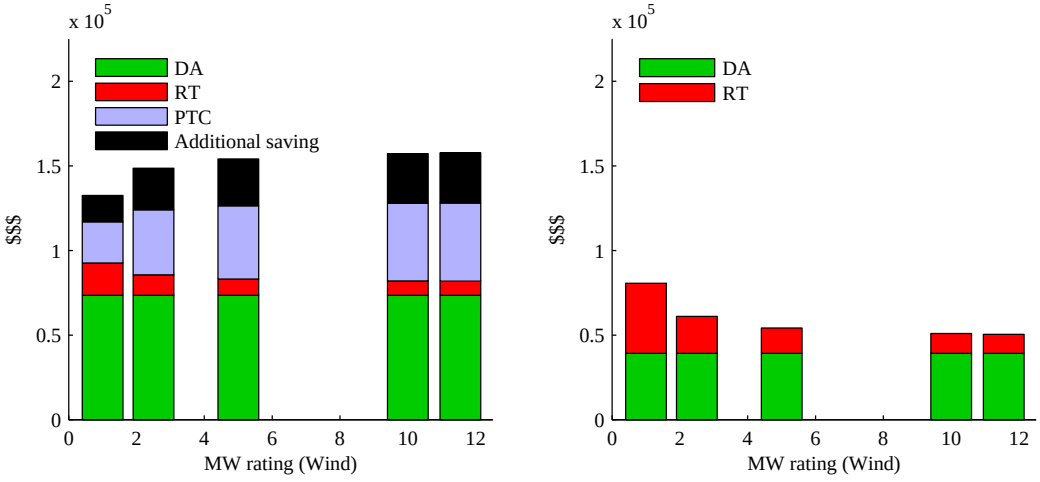

(a) Positive contributors to the value of generation shifting.

(b) Negative contributors to the value of generation shifting.

Figure 2.5: (a) Positive and (b) negative contributors to the value of generation shifting.

The net value is the difference between the aggregated positive contribution and aggregated negative contribution. The net value along with the $/MWh served is plotted in Fig. 2.6(a). The ratio of generation shifted, and the ratio of storage utilized are also plotted alongside in Fig. 2.6(b).

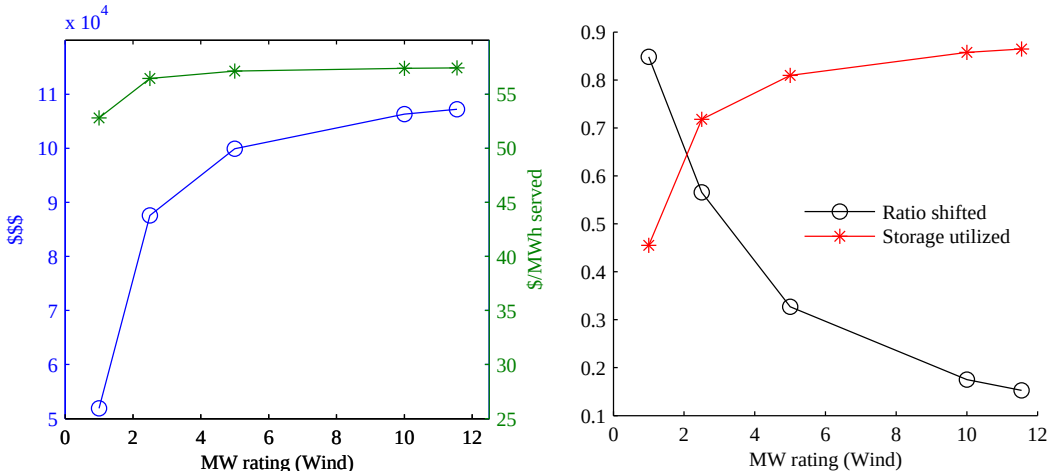

(a) Net value and the $/MWh served against installed wind

(b) Ratio of generation shifted and the ratio of storage utilized against installed wind

Figure 2.6: Results from wind only charging: (a) Net value and the $/MWh served, and (b) ratio of generation shifted and the ratio of storage utilized against installed wind

Discussion

Although the objective is to find the optimal ratio of storage to wind, in this analysis the storage is considered fixed and installed wind is simulated to increase from 1 MW to 11.55 MW. The battery is offered in the DA market as a generator or load without regard to the installed wind. Therefore the positive and negative contribution to the value from DA market is fixed as seen in Fig. 2.5. When the installed wind is low, E_WIND, the energy supplied by wind to charge the battery is also low and therefore the RT_VOL during designated charging period is high. However, with low installed wind it also more likely that the SOC would be deficient (Fig. 2.4(e)) and therefore RT_VOL during designated discharging period is also high — the positive and negative contribution of RT market towards the value of generation shifting is high with low installed wind, most prominently so in the 1:1 storage to wind scenario (Fig. 2.5). It is not desirable to expose the asset to the RT market because of the volatility, and high exposure to RT market is a drawback for low installed wind scenarios.

Furthermore, because of low production owing to lower installed capacity, the PTC

is naturally lower. So are the additional savings because less on-peak energy is displaced by stored wind energy (Fig. 2.5). Consequently, the value of generation shifting is low with lower installed wind as seen in Fig. 2.6(a).

Therefore, on the basis of net value addition and exposure to RT market it seems that a lower storage to wind ratio is favorable.

However, the ratio of shifted generation is significantly better at lower installed wind (Fig. 2.6(b)). This is important because the objective is to enhance the on-peak availability of wind. Larger ratio of shifted generation means higher contributions from the value propositions not considered, e.g. reduced greenhouse emissions and qualification of wind as a reliable resource.

Finally, the value addition per MWh served ($/MWh served) seems to be fairly similar for all scenarios except the 1:1 case in Fig. 2.6(a). If the 1:1 case is not considered any further because of significantly lower value addition in the absolute terms and in terms of per MWh served, the comparison is between the other four scenarios.

Concluding remarks

The 5 MWh installed wind scenario is comparable to even higher wind scenarios in its exposure to RT market and $/MWh served, with only slightly lower net value addition and approximately double the generation shifting. It seems to be a balanced choice with attractive features of both, higher and lower wind scenarios.

The 2.5 MW scenario shifts significantly higher proportion of wind than the 5 MW scenario at similar $/MWh served but at slightly higher exposure to RT market and somewhat lower net value addition. However, it could easily compete if the value from other propositions is included. Therefore the truly optimal scenario would be somewhere in the range of 2.5 MW – 5 MW installed wind per MW storage. Alternatively, the optimal ratio of storage to wind for the sole purpose of shifting wind only generation is 200 – 400 kW storage per MW installed wind, under the obligation that storage should be offered as a generating resource for 6 peak load hours everyday.

Chapter 3

Ramp rate limiting

The objective of this mode was to evaluate the ability of the 1 MW, 7.2 MWh sodium sulfur (NAS) battery to limit the ramp rate of the power output of the 11.55 MW Minwind wind farm. It is desirable for the system operation that the changes in electric power generation be slow and smooth; however, the output of an individual wind farm could vary quite fast as seen in Fig. 3.1.

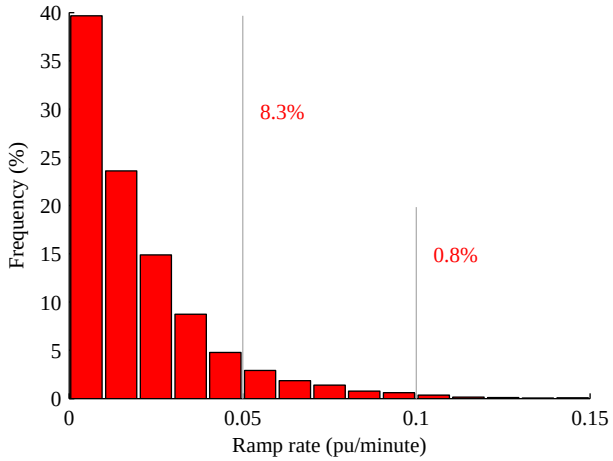

Figure 3.1: Ramp rate of the wind farm. Data corresponds to 12/10/2009 – 12/15/2009 at an approximate resolution of one sample per minute.

One of the techniques to limit the ramp rate is to pass the wind generation time series through a low pass filter and compensate for the difference between the low pass

filter's output and actual wind generation using storage. This amounts to injecting the low pass filter's output into the grid, assuming that the battery can compensate for the difference at all times. It is first shown how the low pass filter's output would have a smaller ramp rate and an upper bound on its ramp rate is established. Later the system is simulated for the verification of this technique.

Low pass filter to limit the ramp rate

Let the per-unit wind generation be represented by $w:\ w(t) \in [0,1]$, and the ramp rate of filtered wind generation by r. Let the time constant of the low pass filter be called T; the low pass filter can be written as,

$$\begin{aligned} H(s) &= \frac{1}{sT+1} \\ h(t) &= \frac{e^{-t/T}}{T} u_s(t), \quad u_s(t) \text{ is unit-step} \end{aligned} \tag{3.1}$$

Also,

$$\mathcal{L}\{w(t)\} = W(s)$$

The "filtered" wind power output is $H(s)W(s)$. Ramp rate of the filtered output, $r(t)$, is the derivative of $h(t) * w(t)$, or equivalently $R(s) = sH(s)W(s)$ (in frequency domain). '$*$' denotes the convolution operation.

$$\begin{aligned} R(s) &= sW(s)H(s) \\ &= \frac{sW(s)}{sT+1} \\ &\equiv \underbrace{\frac{s}{sT+1}}_{:=G(s)} \times W(s) \end{aligned} \tag{3.2}$$

Unfiltered wind generation w is the input to the system G defined in (3.2), and the output of this system is the ramp rate, r.

$$\begin{aligned} G(s) &= \frac{s}{(sT+1)} \\ &= 1/T\left(1 - \frac{1}{sT+1}\right) \\ \Rightarrow g(t) &= \mathcal{L}^{-1}\{G(s)\} \\ &= \frac{1}{T}\left(\delta(t) - \frac{1}{T}e^{-t/T}u_s(t)\right) \end{aligned} \tag{3.3}$$

$$\begin{aligned} R(s) = G(s)W(s) &\xrightarrow{\mathcal{L}^{-1}} g(t) * w(t) \\ &= \int_{-\infty}^{\infty} g(t-\tau)w(\tau)d\tau \\ &= \frac{1}{T}\int_{-\infty}^{\infty}\left(\delta(t-\tau) - \frac{1}{T}e^{-(t-\tau)/T}u_s(t-\tau)\right)w(\tau)d\tau \\ &= \frac{1}{T}\left(\int_{-\infty}^{\infty}\delta(t-\tau)w(\tau)d\tau - \int_{-\infty}^{\infty}\frac{1}{T}e^{-(t-\tau)/T}u_s(t-\tau)w(\tau)d\tau\right) \\ &= \frac{1}{T}\left(w(t) - h(t) * w(t)\right), \quad \text{where } h \text{ is the system in (3.1)} \end{aligned} \tag{3.4}$$

From the theory of linear systems,

$$\begin{aligned} |r(t)| &\leq \frac{1}{T}\left(\|w\|_\infty + \|w\|_\infty \int_{-\infty}^{\infty}|h(t)|\,dt\right) \\ &= \frac{2}{T}\|w\|_\infty \end{aligned} \tag{3.5}$$

Since $\|w\|_\infty = 1\text{pu}$, the absolute ramp rate of the output is bounded by $2/T$ where T is the chosen time constant.

3.1 Simulation of ramp rate limiting

Fig. 3.2 shows the block diagram of the system. In addition to the ramp rate limiting section, there is a proportional controller to keep the SOC at the desired setpoint. The controller constant must keep the SOC close to the setpoint but at the same time it must not result in excessive control effort. Minimizing the disturbances in SOC is advantageous because it leaves the energy stored in the battery available for other

applications as described later. The sub-unity battery efficiency is not considered in this analysis because the closed loop SOC controller can compensate for it.

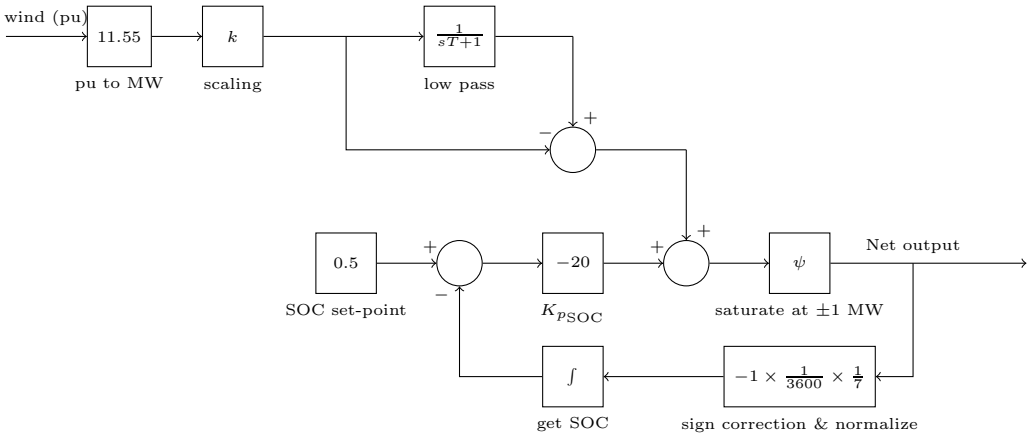

Figure 3.2: Block diagram for simulating ramp rate limiting

Simulations indicate that the upper bound on the ramp rate obtained from the preceding analysis might be too high for practical purposes. While a time constant chosen according to this upper bound should theoretically work, the control effort requested would be too high, at times violating the ±1 MW limit on the battery output. Fig. 3.3 shows the ramp rate of the unfiltered wind farm generation, theoretical ramp rate of the low pass filtered output, and the ramp rate of the simulated output of the system with power and energy constraints applied when the time constant was chosen to limit the ramp rate to 0.05 pu/minute.

It is seen that while the ramp rate of the ideal output is well below the desired limit, the ramp rate of the actual output occasionally exceeds the limit. Fig. 3.4 shows the plot of battery power output and SOC for this case, and it is clear that the violations in the ramp rate are not because of the battery reaching its energy limit, but because of the high control effort (power) requested.

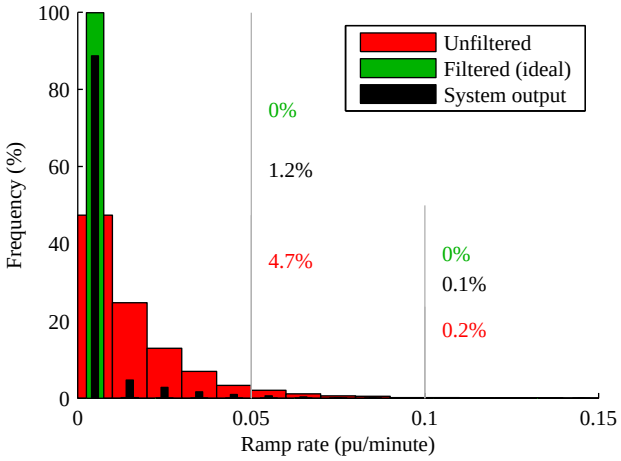

Figure 3.3: Ramp rate with $T = 2400\,\mathrm{s}$

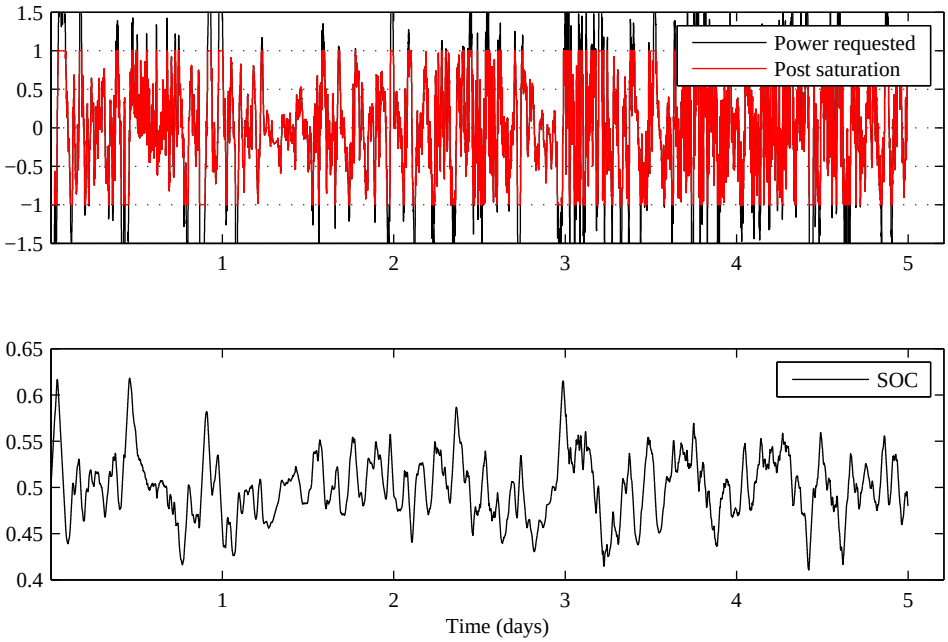

Figure 3.4: Battery power and SOC with $T = 2400\,\mathrm{s}$

To alleviate this problem, it is necessary to reduce the time constant below the theoretically obtained number and simulate with different values to achieve an acceptable limit. For a limit of 0.05 pu/minute, the simulations indicate that a time constant of 120 (2 minutes) keeps the system ramp rate under limit most of the times. Fig. 3.5 shows the ramp rates of the generation, ideal output and actual output for this time constant. It is seen that the performance is in fact slightly better than the $T = 2400$ case. Also, as seen from Fig. 3.6, the control effort rarely exceeds the ± 1 MW limit. Finally, with the lower time constant, the SOC is confined to a much tighter band (compare Figs. 3.4 and 3.6)

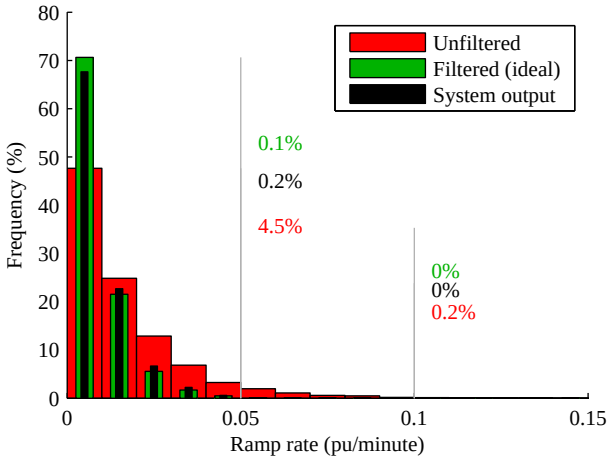

Figure 3.5: Ramp rate with $T = 120\,\mathrm{s}$

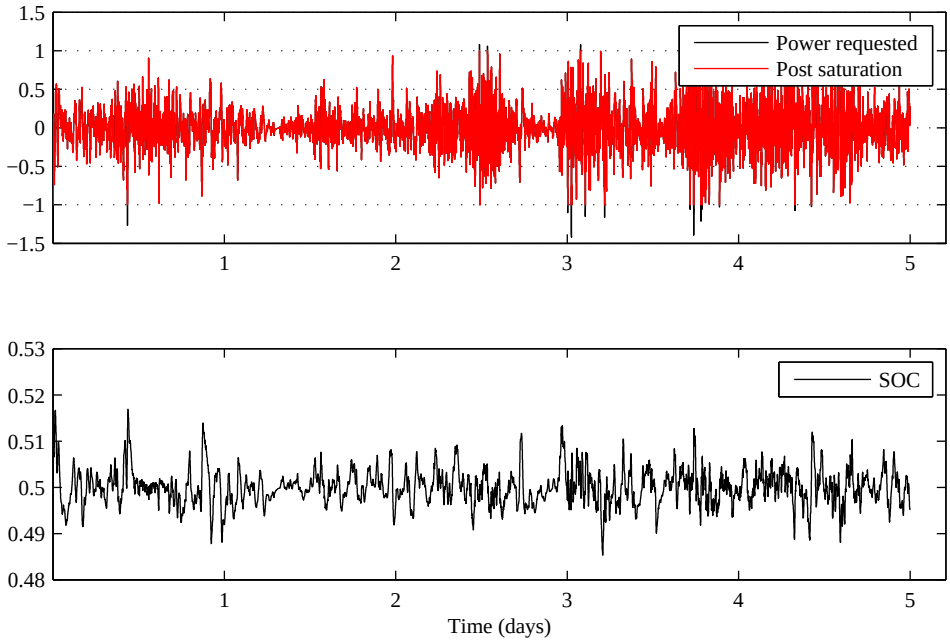

Figure 3.6: Battery power and SOC with $T = 120\,\mathrm{s}$

3.2 Results from the actual system operation

3.2.1 Part I

Simulation results presented above indicate that a time constant of 120 seconds keeps the violations of the 0.05 pu/minute ramp rate limit reasonably low. The system was run with this time constant and data was collected at a resolution of 1 minute for one week beginning 05/29/2011. The ramp rates are plotted in Fig. 3.7

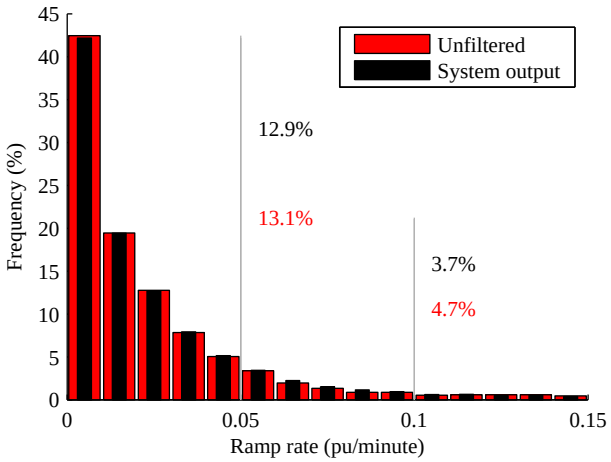

Figure 3.7: Ramp rate from the actual runs of the system with $T = 120\,\mathrm{s}$

The ramp rate of the system output is no better than the ramp rate of unfiltered generation; this is in stark contrast against the simulation results using the same data and time constant setting plotted in Fig. 3.8. It is clear that the system operation does not correspond to the block diagram of Fig. 3.2, which it ideally should. This is also evidenced from the plot of battery power (Fig. 3.9) during the period of study.

More data was collected at a larger time constant and finer resolution (10 s). However, there was no improvement in the output ramp rate and the battery exhibited periods of inactivity similar to Fig 3.9. The block diagram simulated was verified to be correct by S&C[1] and we believe that the problem lies with its implementation. The issue stands unresolved as of now.

[1]S&C Electric designed and manufactured the power conversion system (PCS) and the associated software.

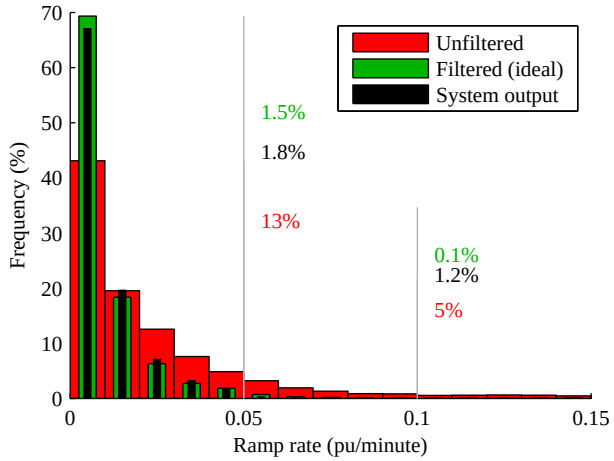

Figure 3.8: Ramp rate from simulation using data and settings of Fig. 3.7

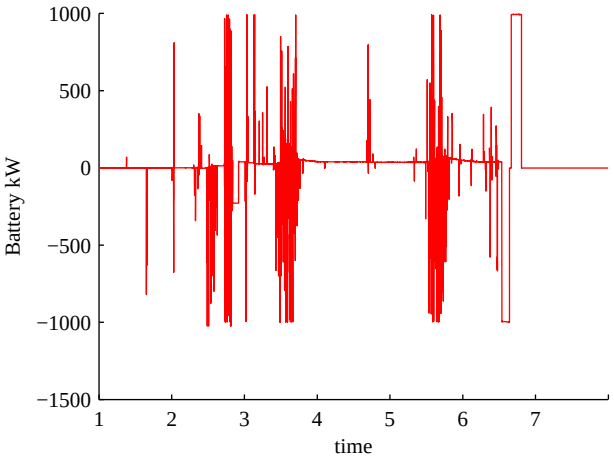

Figure 3.9: Battery power during testing the ramp rate limiting (Part I)

3.2.2 Part II

Although the assertion that a time constant much smaller than the one theoretically obtained would suffice could not be verified because of unresolved issues, other experimentally obtained data sets exist that establish the validity of simulation results.

The information from one of such data sets corresponding to an approximately 16 hour long interval during 01/31/2010 – 02/01/2010 is now presented. The scaling factor was set to 0.433 to emulate a 5 MW installed wind scenario; a time constant of 1200 s (20 minutes) was used. Theoretically the ramp rate would always be bound by 0.1 pu/minute with this time constant, provided that the battery can always source/sink the requested power. The unfiltered generation, compensation from storage and the total system output is plotted in Fig. 3.10. The total output is visibly smooth. The ramp rates of the unfiltered generation and the total system output are shown in Fig. 3.11(a). The ramp rates obtained from simulation using the same generation data under the same settings are shown in Fig. 3.11(b).

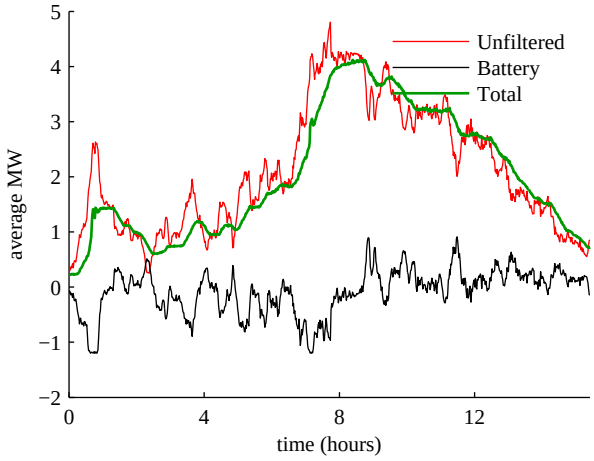

Figure 3.10: Unfiltered generation, compensation from the battery, and the total power output with 5 MW installed wind scenario and $T = 1200$ s

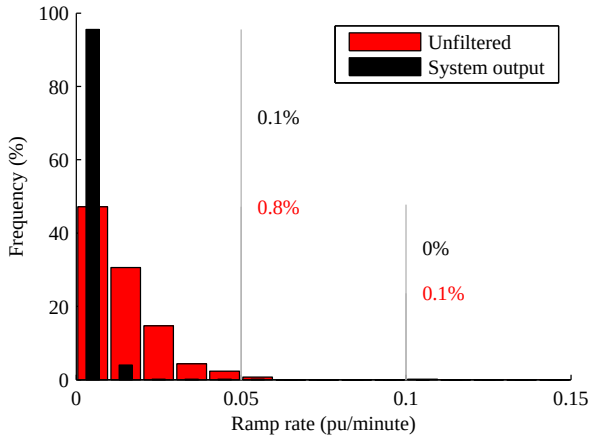

(a) Actual ramp rates of the system with $T = 1200\,\mathrm{s}$

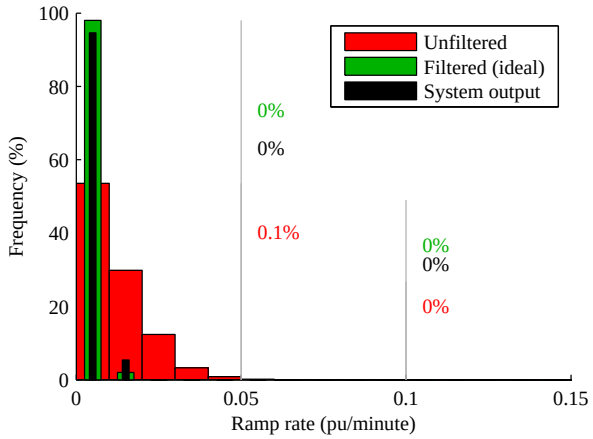

(b) Ramp rate from simulation using data and settings of Fig. 3.11(a)

Figure 3.11: (a) Actual and (b) simulated ramp rates for an effective 5 MW wind scenario with $T = 1200\,\mathrm{s}$

Key observations

- The battery is able to limit the ramp rate effectively.
- The total ramp rate is restricted to a value significantly smaller than the analytical upper bound.
- There is very good correspondence between the simulated and actual results.
- The slight differences between the actual results and the simulation are attributed to the simulation program used: MATLAB/Simulink chooses the time step automatically and uses interpolation that might result in slight softening of the ramp rates.

3.3 Extended simulation results

With confidence in the simulation model, different scenarios were simulated using generation data from the Minwind wind farm for the year 2007 at a resolution of 1 minute. The unfiltered ramp rates for this data are plotted in Fig. 3.12. A total of 30 cases were simulated with the time constants (minute) varying in $\{2, 5, 10, 20, 40, 80\}$, and the installed wind (MW) varying in $\{1, 2.5, 5, 10, 11.55\}$ for a period spanning an year, totaling a simulated time of 30 years. It is expected that the year long simulations would average out the seasonal variations in the wind.

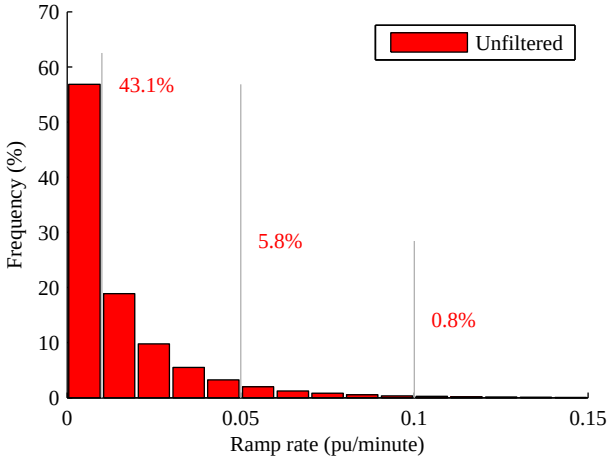

Figure 3.12: Ramp rates for the Minwind wind farm for the year 2007

The results from simulations are tabulated in Table 3.1. It is seen that storage succeeds in mitigating the ramp rates of Fig. 3.12 in all cases. However, the effectiveness of storage depends upon the time constant and the installed wind — with higher installed wind and at higher time constants, the violations in the ramp rates at all limits (0.01, 0.5, and 0.1 pu/minute) tend to increase. Even though the results are always better than the unfiltered generation, it is not hard to see that increasing the time constant beyond a limit is contrary to its intended purpose.

The explanation for this unintended behavior is the limited MW capability of the storage, as discussed earlier in the context of Figs. 3.3 and 3.4. It was also seen that the performance is independent of the battery MWh capacity, provided the MWh capacity

is sufficiently large, as is the case for the NAS battery in question.

Therefore the optimal storage MW/wind MW ratio for ramp rate limiting would depend upon the time constant chosen. Alternatively, the ratio could be picked from Table 3.1 once the specifications on the allowable ramp rates are set.

Installed wind (MW)	Time constant (min)	% exceedance at 0.01 (pu/min)	0.05 (pu/min)	0.1 (pu/min)
11.55	2	25.37	0.63	0.23
	5	15.88	0.95	0.26
	10	10.03	1.22	0.29
	20	7.72	1.46	0.31
	40	8.71	1.68	0.33
	80	10.05	1.85	0.35
10	2	25.41	0.6	0.16
	5	16.1	0.7	0.21
	10	10.28	0.93	0.24
	20	6.8	1.14	0.25
	40	6.72	1.33	0.27
	80	7.72	1.48	0.29
5	2	25.46	0.76	0.04
	5	16.43	0.14	0.05
	10	11	0.17	0.07
	20	6.94	0.23	0.08
	40	4.31	0.29	0.09
	80	2.85	0.33	0.09
2.5	2	25.46	0.77	0.05
	5	16.45	0.19	0.01
	10	11.08	0.06	0.01
	20	7.11	0.03	0.01
	40	4.55	0.03	0.02
	80	3.12	0.04	0.02
1	2	25.48	0.79	0.07
	5	16.49	0.21	0.02
	10	11.13	0.09	0
	20	7.17	0.03	0
	40	4.62	0.01	0
	80	3.19	0	0

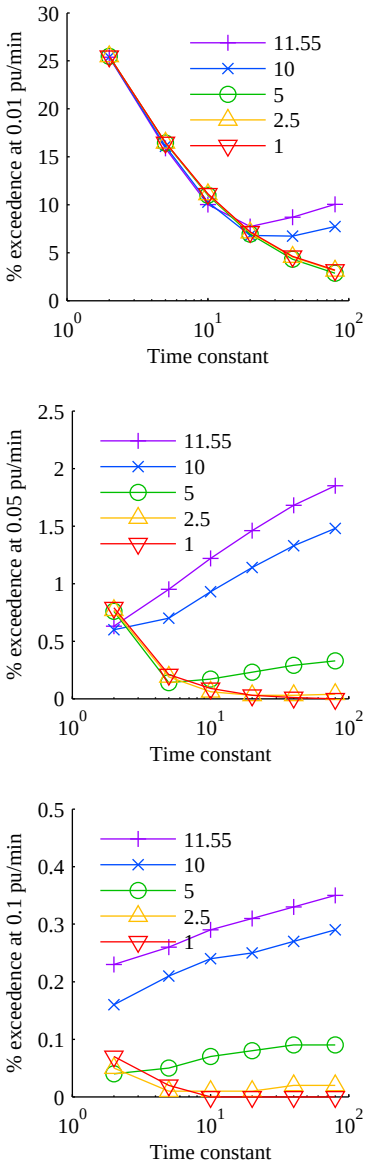

Table 3.1: Extended simulation results in tabular and graphical format. The effect of insufficient storage MWs is seen at higher time constants and higher installed wind cases: the entries in red correspond to the cases when violations in the ramp rate start to increase upon increasing the time constant.

3.4 Ramp rate limiting as a secondary function

It is seen from Fig. 3.6 that the battery SOC is confined to a tight band. If the SOC setpoint in the block diagram of Fig. 3.2 is replaced by an appropriate time varying SOC profile, it should be possible to have the battery shift the wind generation while limiting the ramp rate.

Simulation with the SOC setpoint replaced by an appropriate SOC profile was carried out and the ramp rates were recorded. The results are plotted in Fig. 3.13. The battery SOC is plotted in Fig. 3.14(a) and the battery power output is plotted in Fig. 3.14(b).

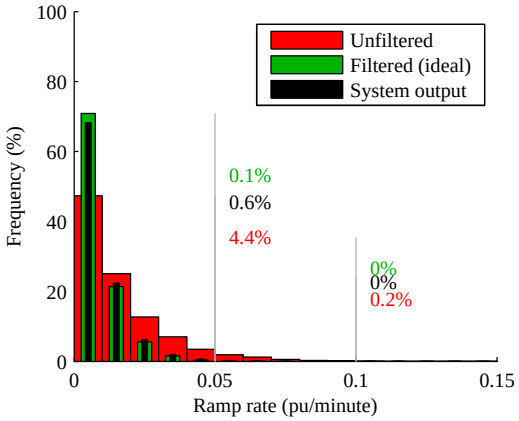

Figure 3.13: Ramp rate with $T = 120\,\mathrm{s}$ with basic GS combined. Effective wind farm rating = 5 MW

The time constant was set to 120 (2 minutes), and the scaling factor was set to 5/11.55 to simulate an effective 5 MW installed wind scenario. The efficiency of the battery was set to 85% and was assumed to be distributed geometrically between charging and discharging similar to Section 2.2. The wind generation data was from the month of December and the designated charging and discharging periods were chosen from Table 2.1.

It is seen that the battery is able to perform both functions simultaneously. For the case presented, the SOC is varied between 0.1 and 0.9. It is possible to go further up (and down). However, to combine the two modes it is important leave some margin

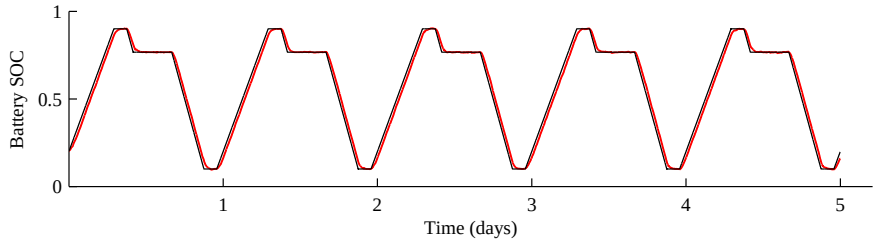

(a) SOC with $T = 120\,\mathrm{s}$ with basic GS and ramp rate limiting combined.

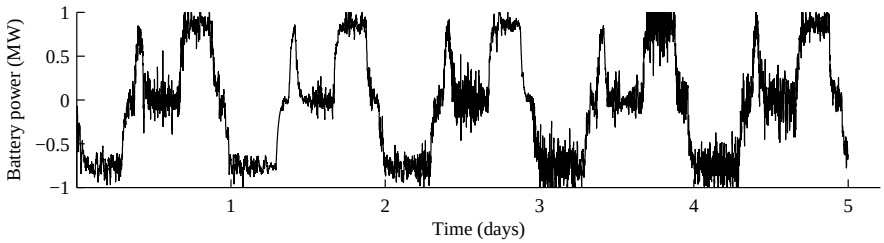

(b) Battery power output with $T = 120\,\mathrm{s}$ with basic GS and ramp rate limiting combined.

Figure 3.14: (a) The battery SOC (red) and the basic GS reference (black), and (b) the battery power output plotted against time.

(dependent upon the time constant) at the limits so that the battery can sink/source energy when requested to do so by the ramp rate limiting part of the system. It should be noted that when the battery is charging and discharging under basic GS, there would be competition between the two objectives and the performance could suffer. Fig. 3.15 shows the results with and without combining the two objectives at different time constants for a 5 MW installed wind scenario.

For all the time constants combining the two modes results in some loss in performance. The loss in performance is more severe at higher time constants. The loss is insignificant at higher limits (0.05 pu/min, 0.1 pu/min) but is noticeable at lower limits (0.01 pu/min). Therefore, if it is desired to keep the ramp rates under 0.05 pu/min most of the time, then the two functions can be easily integrated. However, if the limit on the ramp rate is tighter, then the basic GS specifications need to be relaxed by lengthening the designated charging and discharging periods: for a longer designated charging, the power requirement *only* to charge the battery would be lower leaving more

room for ramp rate limiting. Because of the presence of a nonlinear saturation element and because of the fact that wind is stochastic as opposed to deterministic, the optimal solution can be more easily determined by simulation with the following parameters available for tuning:

1. The time constant T,
2. The length of the designated charging/discharging period, and
3. The gain of the proportional controller.

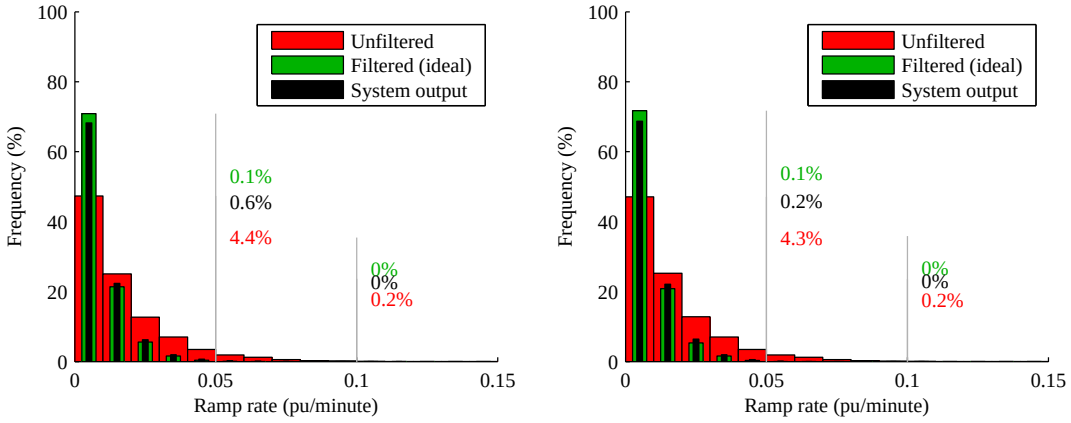

(a) Ramp rates with basic GS combined. $T = 120$ (b) Ramp rates without basic GS combined. $T = 120$

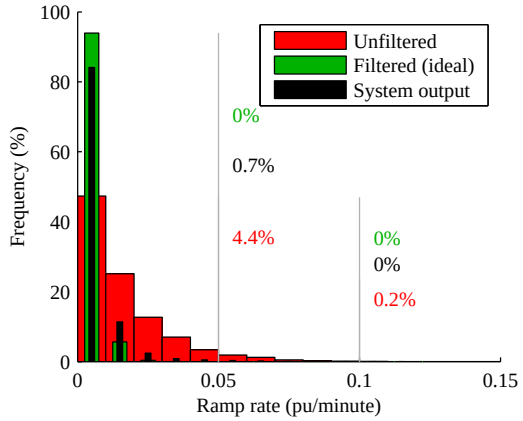

(c) Ramp rates with basic GS combined. $T = 600$

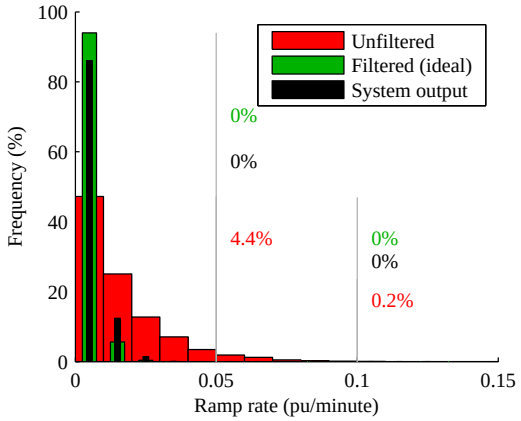

(d) Ramp rates without basic GS combined. $T = 600$

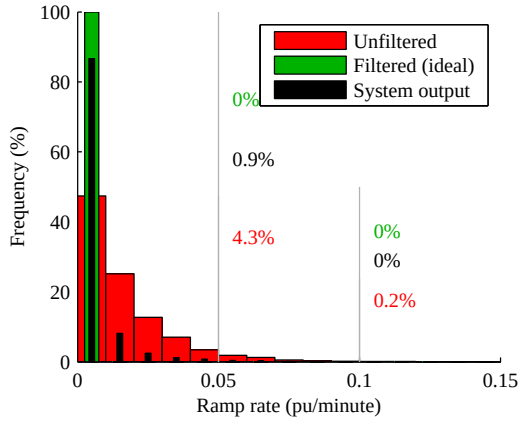

(e) Ramp rates with basic GS combined. $T = 3000$

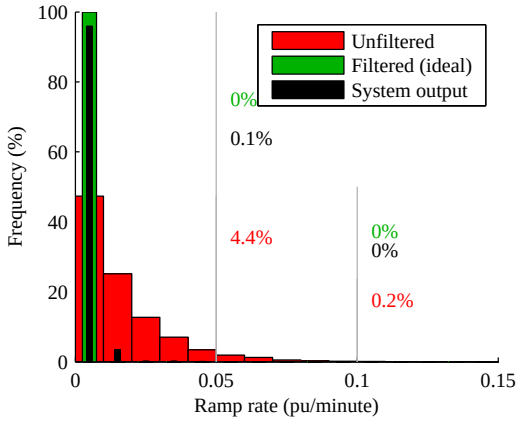

(f) Ramp rates without basic GS combined. $T = 3000$

Figure 3.15: Ramp rates with and without combining basic GS with ramp rate limiting, at different time constants for an effective 5 MW installed wind scenario and the battery round trip efficiency equal to 85%

Concluding remarks

The battery's ability to limit the ramp rate of wind generation effectively has been verified in practice. Furthermore, the validity of simulation model to study the ramp rates has been established by the experimental results.

Analytical justification for the low pass filter based technique for ramp rate limiting has been provided. At the same time it is shown that the recommended time constant from the analytical bound could be excessive and even impractical.

It is also shown that multiple modes of operation could be combined to enhance the value from the battery storage. Furthermore, the limiting factor in the 11.55 MW scenario was the MW rating of the battery (Fig. 3.4). From the results of the previous section (basic generation shifting: wind only charging), it was concluded that the storage to wind ratio should be in the 20% – 40% range (MW/MW). For this ratio, more storage MWs would be available and the battery would be able to control the ramp rate more effectively. This is also seen in Fig. 3.11 (20% storage MW/wind MW) where the ramp rates of the ideal output and the system output are very close, and in Table 3.1 where increasing the storage/wind ratio beyond 20% – 40% (MW/MW) results in only insignificant increase in performance.

Therefore the optimal storage to wind ratio for generation shifting would also be suitable for limiting the ramp rate of wind generation. Moreover, these two tasks could be combined for maximum benefit to the system.

Chapter 4

A statistical model for wind power forecast error

In the last chapter the ability of the battery to compensate for the minute-to-minute variations in wind generation was studied. Energy storage could also be used to compensate for the forecast errors in wind. Although traditional generation has the potential to absorb the forecast errors, the compensation would come at the cost of efficiency, and would cause pollution and rotor fatigue as argued in the Introduction.

Different methods for forecasting wind exist for different forecast horizons. The long term forecasts use highly sophisticated models that make the best use of Numerical Weather Prediction (NWP) and statistical methods [37–39]. In spite of these developments, Persistence, the simplest and cheapest forecast method, continues to perform at par, if not outperform, the more advanced models at forecast horizons shorter than a few hours [39–43].

Forecasts are not perfect and there always are some errors. A probabilistic methodology to estimate the costs associated with prediction error has been presented in [44]. Optimal bidding strategies based on forecast uncertainty have been formulated in [45] and storage sizing based on an energy rejection limit has been described in [46]. The net forecast error could also be used to determine the type and the amount of reserves to be carried on the system level. The forecast error is generally assumed to be Normally distributed, and determination of reserves based on this assumption has been reported

in the literature [8, 9, 47, 48]. Optimal allocation of standing and spinning reserves and an analysis of the value of bulk energy storage based on the Normal assumption with a slight modification have been presented in [49]. In [50], the author has made the Normal assumption for wind speed forecast error and has found the wind power forecast error distribution for an individual site by a nonlinear transformation. However, the net system error is finally assumed to be Normally distributed. The Normal assumption has been challenged in few works and researchers have proposed a weighted sum of beta distribution functions as a more suitable distribution function [46, 51, 52].

The focus of the presented analysis is only on the error from the Persistence forecasts. The Persistence method and its relevance is discussed first, followed by a discussion on the existing models. It is shown that an alternative could be to model the error by a mixed distribution as opposed to a continuous distribution. A mixed distribution function based on the Laplace distribution is proposed. This model is then used to calculate the penalties for departure from a schedule submitted based on forecasts, and hence estimate the returns from the storage installed to compensate for the departure from the forecast value. Finally, it is shown using simulated data from several locations that the independence of the forecast errors arising from geographical dispersion would cause the net forecast error to follow a Normal distribution as reasoned in [53]. Therefore, the usefulness of the proposed model would be at the level of market participation of an individual wind farm, and the Normal approximation would suffice at the level of Reliability regions.

4.1 Persistence for forecasting wind generation

The Persistence method is based on the fact that the atmosphere could be considered 'quasi-stationary' on a time scale of few hours [41], and hence wind generation could be assumed to vary slowly enough, such that the average power over the most recent time step can be used as a forecast for the average power k time steps ahead. Let P_i denote the average power over an interval $\mathbb{T}_i$ of length T_p, the forecast period. Also, let $\widehat{P}$ denote the forecasted value of the average power. According to the Persistence method

$$\widehat{P}_{i+k+1} = P_i \tag{4.1}$$

In the above expression, the forecast horizon is the time from the instant of forecast until the beginning of the time interval for which forecast is being made. The forecast horizon, kT_p, should typically be less than 6 hours which is considered as the limit of purely statistical forecasting methods [43]. The forecast error for a given interval is,

$$e(t) = P_i - \widehat{P}_i, \qquad t \in \mathbb{T}_i \tag{4.2}$$

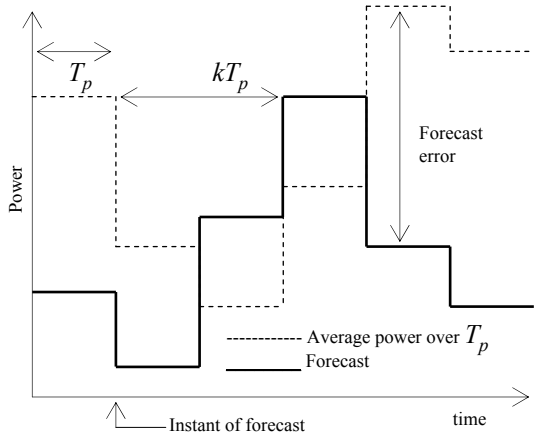

Figure 4.1: The Persistence method

Fig. 4.1 illustrates the Persistence forecast. As pointed out, Persistence, even though the simplest, is a credible forecast strategy at forecast horizons up to a few hours. For this work, forecast horizons less than or equal to 6 hours are used. This time scale is certainly convenient for trading in the short term markets; for the DA markets, NWP based forecasting techniques are more appropriate. Energy, not power, is the quantity traded; therefore the forecast error in the *average* power, as indicated in Fig. 4.1 and defined in (4.2), is used for this work.

4.2 Need for an accurate model, existing models and the data used

4.2.1 Need for an accurate model

Let's denote the actual Probability Density Function (pdf) of the wind power forecast error by f_e, and the approximated pdf by $\widehat{f}_e$. The corresponding cumulative distribution functions (cdfs) would be F_e and $\widehat{F}_e$. Let the pdf and cdf for the load forecast error be f_L and F_L. If the model is being used to size an energy storage on the basis of the energy rejection limit as proposed in [46], there will be an error $\Delta E_{rejected}$ in the estimation of the rejected energy:

$$\Delta E_{rejected} = \frac{1}{\overline{P}} \int_{P_{ESS}}^{1} \left(\widehat{f}_e(e) - f_e(e) \right) (e - P_{ESS})\, de \tag{4.3}$$

where $\overline{P}$ is the long term mean of generated energy, P_{ESS} is the maximum power that the energy storage can draw, and e is the forecast error. $\Delta E_{rejected}$ would be obtained as a fraction of the total energy generated from (4.3).

Similarly, if the model is being used to compute the reserve requirements that will ensure system security with a certain probability, considering the wind power forecast error and the load forecast error only, the net (wind + load) forecast error, e_{sys}, would have a pdf f_{sys} given by,

$$\begin{aligned} f_{sys}(e_{sys}) &= (f_e * f_L)(e_{sys}) \\ &= \int_{-\infty}^{\infty} f_e(x)\, f_L(e_{sys} - x)\, dx \end{aligned} \tag{4.4}$$

and the error, $\Delta \mathrm{Pr}_{sec}(P_r)$, in computing the probability that system would be secure with P_r reserves would be,

$$\begin{aligned} \Delta \mathrm{Pr}_{sec}(P_r) = \int_{-\infty}^{P_r} \int_{-\infty}^{\infty} &\left(\widehat{f}_e(x) - f_e(x) \right) \\ &\times f_L(e_{sys} - x)\, dx\, de_{sys} \end{aligned} \tag{4.5}$$

The two examples above show that the model pdf $\widehat{f}_e$ should be close to the actual pdf f_e to minimize the error in the computation of the storage requirements, and the reserves. Similar reasoning could be extended to other analyses pertaining to the calculation of integration costs.

It should be noted that f_e is the pdf of forecast error over all values of forecast. It is possible, and in many cases desirable [45], to include uncertainty for every value of forecast. However, the model and case study discussed in this paper do not require an assessment of uncertainty for every value of forecasted power.

4.2.2 The Normal approximation to forecast error

Forecast error is generally assumed to follow a Normal distribution with parameters estimated by Maximum Likelihood Estimation (MLE):

$$\widehat{\mu}_e = \frac{1}{n}\sum_{i=1}^{n} e_i \tag{4.6}$$

$$\widehat{\sigma}_e^2 = \frac{1}{n}\sum_{i=1}^{n} (e_i - \widehat{\mu}_e)^2 \tag{4.7}$$

Fig. 4.2 shows the pdf of the forecast error and the corresponding Normal fit, plotted using the data set 1.2004. Forecast period and forecast horizon, both, are 1 hour. Although, it seems that the pdfs converge in the tails, it will be shown later that departure from normality is much more pronounced in the tails.

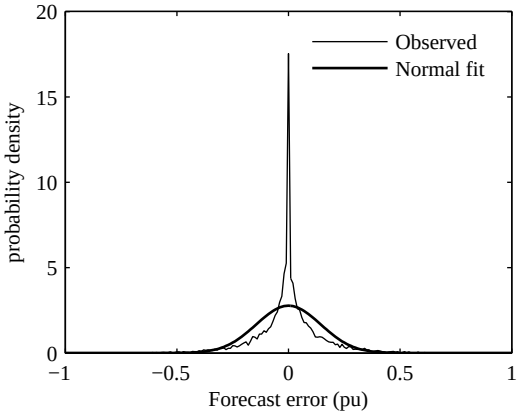

Figure 4.2: pdf of wind power forecast error for a forecast period of 1 hour and a forecast horizon of 1 hour, and for corresponding Normal fit, using dataset 1.2004

4.2.3 The weighted beta distribution model

The probability density function for beta distribution is given by

$$f_{\alpha,\beta}(x) = \frac{\Gamma(\alpha+\beta)}{\Gamma(\alpha)\Gamma(\beta)} x^{\alpha-1}(1-x)^{\beta-1}, \quad x \in (0,1) \tag{4.8}$$

The weighted beta distribution model is based on the reasoning that the observed wind power values corresponding to a given forecast can be modeled by a beta distribution. If the forecasts are sorted into n number of bins such that the predicted power corresponding to i-th bin is $\widehat{P}_i$, then the pdf of the observed power would be $\widehat{f}_{\alpha_i,\beta_i}$. Depending upon the frequency of each forecast bin, it can be assigned a weight w_i. The pdf of error could then be estimated as

$$\widehat{f}_e(e) = \sum_{i=1}^{n} w_i \times \widehat{f}_{\alpha_i,\beta_i}(e + \widehat{P}_i) \tag{4.9}$$

Figures 4.3(a) and 4.3(b) show the empirical and the modeled pdfs of observed power corresponding to a forecasted power of 0.9 pu and 0.5 pu. The forecast period and the forecast horizon, both, are 1 hour, although both may vary independently. Persistence forecast was used; the data sets span 1 year, and are from different sites. To estimate the parameters α and β, the function `betafit` built into the Statistics Toolbox of MATLAB [54] was employed which uses Maximum Likelihood Estimation.

It can be seen that the probability density approaches ∞ at the bounds in the above cases. This would translate into an infinite probability density at $e = 0.1$ pu for data set 1.2004 and at $e = \pm 0.5$ pu for data set 2.2004 for any finite value of corresponding weights, which is contrary to the typical distribution of forecast errors for Persistence. Note that limited number of data points is not a reason for this anomaly. Therefore, even though beta pdf has attractive properties like a variable shape, a variable kurtosis, and a relevant domain of definition, it cannot be used to model the observed power for the purpose of generating the forecast error pdf at the forecast horizons and the data sets examined.

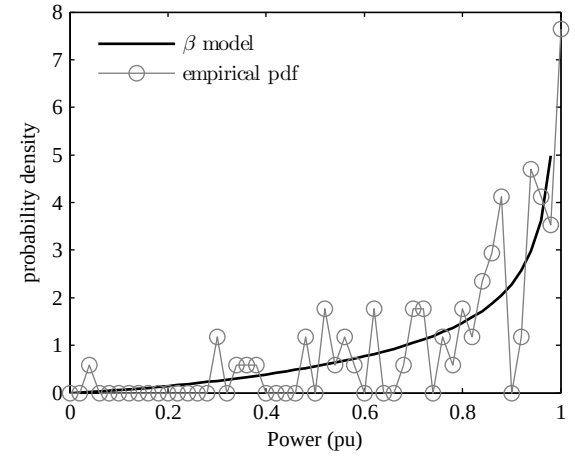

(a)

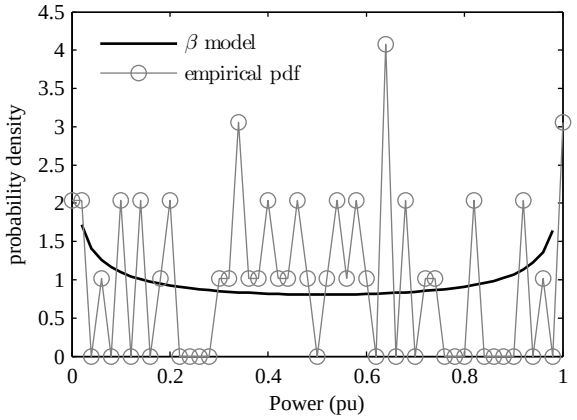

(b)

Figure 4.3: Empirical and beta modeled pdfs for forecast (a) $\widehat{P} = 0.9$ pu using data set 1.2004, and (b) $\widehat{P} = 0.5$ pu using data set 2.2004. Forecast period 1 hour, forecast horizon 1 hour.

4.2.4 Data used in this study

The data used for this work is from the Western Wind Resources data sets designed by 3TIER in association with National Renewable Energy Laboratory (NREL). The data sets contain wind speed and wind power output from hypothetical wind farms, each rated 30 MW, at a temporal resolution of 10 minutes. "This data set was designed to help energy professionals perform wind integration studies, compare potential wind sites spatially and temporally, and estimate power production from hypothetical wind plants." The details are provided in [55]. Data sets correspond to the years 2004, 2005 and 2006. Data from 20 sites is used and the sites are numbered 1 through 20 as shown in Fig. 4.4. Accordingly, data from a site 's' for year 200n is called data set s.200n in this paper.

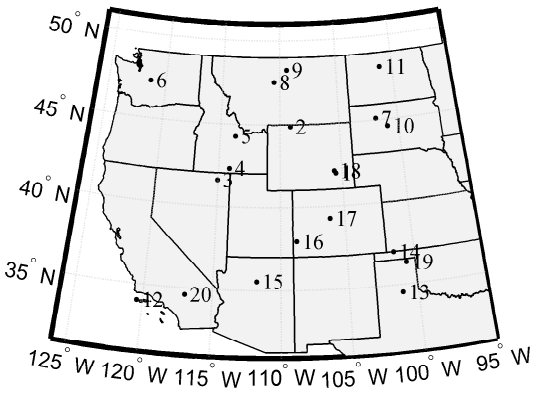

Figure 4.4: Sites used to study the distribution of forecast error

Data for the electricity prices corresponds to the Real Time Locational Marginal Prices (RTLMPs) for the MINN.HUB of the Midwest ISO.

4.3 The discrete nature of wind power forecast error and a mixed distribution

4.3.1 Discreteness in the wind power forecast error

Fig. 4.5 shows the distribution of wind speeds with the power curve of a generic wind turbine superimposed. The cut-in speed is 3 ms^{-1}, the rated speed is 15 ms^{-1}, and the cut-out speed is 25 ms^{-1}. The power output varies continuously between the cut-in speed and the rated speed, but is always zero below the cut-in speed and above the cut-out speed, and is at its rated value between the rated speed and the cut-out speed. It can be seen that the power output can stay constant (at 0 pu or 1 pu) even with significant variations in wind speed, and the relation between power output and speed is nonlinear. Therefore, even though wind speed can be modeled as a Weibull distributed random variable, which is a special case of extreme value distribution, it is not possible to use a similar distribution for wind power, and the associated error.

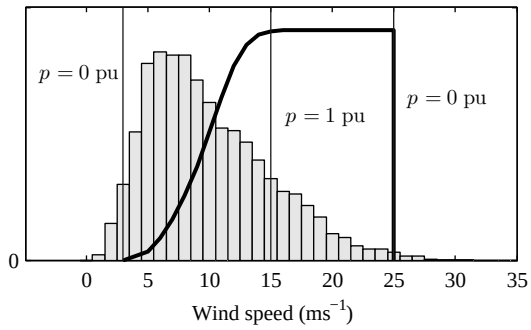

Figure 4.5: Distribution of wind speeds from data set 1.2004 with a generic power curve superimposed

Let's consider a case in which the power output is 1 pu for several hours. The wind speed still varies, but between the rated speed and the cut-out speed. The instantaneous power thus equals the average power over this period which could easily be a few hours. It is not hard to see that the forecast error would be equal to zero for a significant amount of time, were such a case to occur. The situation would be similar for speeds consistently low enough or high enough such that the turbine/farm produces no power.

The forecast error would, in fact, be zero whenever Persistence correctly predicts the average power output, with majority of these cases occurring when the power output stays constant over an extended period of time. Table 4.1 shows the probability of error being equal to zero for several data sets. Other values of error are also evaluated for comparison. All errors less than 0.001 pu are taken to be 0.

data set	$\Pr(e = 0)$	$\Pr(e = 0.1)$	$\Pr(e = 0.2)$
1.2004	0.10	0.00	0.00
1.2005	0.10	0.00	0.00
2.2004	0.20	0.00	0.00
2.2005	0.20	0.00	0.00

Table 4.1: Probabilities of observing different values of error for a forecast period of 1 hour and a horizon of 3 hours for different data sets

It is evident that the error e behaves like a continuously distributed random variable for the most part but has a point probability at 0. This characteristic can not be captured by any continuous distribution function and it seems natural to resort to a mixed distribution function.

4.3.2 A mixed distribution function for the wind power forecast error

Let the probability of the forecast error being equal to 0 pu be π_0.

$$\Pr(e = 0) = \pi_0 \tag{4.10}$$

Then the pdf of the forecast error can be written as,

$$f(e) = (1 - \pi_0) f_c(e) + \pi_0 \delta(e) \tag{4.11}$$

f_c is the continuous part of the pdf and δ is the Dirac delta function. The subscript e has been dropped for the ease of notation. The cdf can be written as

$$F(e) = (1 - \pi_0) F_c(e) + \pi_0 H(e) \tag{4.12}$$

where H is the Heaviside step function defined in the following way

$$H(e) = \begin{cases} 0, & \text{if } e < 0 \\ 1, & \text{if } e \geq 0 \end{cases} \tag{4.13}$$

The point probability at $e = 0$ has been calculated as

$$\pi_0 = \Pr(|e| \leq 0.005) \tag{4.14}$$

Once the data points within ± 0.005 were removed, rest of the data was modeled using the Laplace distribution. Arriving at this distribution was a trial and error process based on similarity in shape of the distribution. The pdf of this distribution is given by

$$f(x) = \frac{1}{2\,b} \exp\left(-\frac{|x - \mu|}{b} \right), \quad x \in \mathbb{R} \tag{4.15}$$

The parameters μ and b can be estimated using MLE as

$$\widehat{\mu} = \text{median}(e) \tag{4.16}$$

$$\widehat{b} = 1/n \sum_{i=1}^{n} |e_i - \widehat{\mu}|, \qquad |e_i| \geq 0.005 \tag{4.17}$$

Fig. 4.6 shows the empirical cdf along with the cdfs from the proposed model, and from the Normal approximation for the data set 1.2005. Forecast period and horizon, both, are 1 hour for consistency with Fig. 4.2. cdfs, rather than pdfs are shown because

mixed distribution functions are better represented by cdfs. It is hard to decipher any difference between the empirical cdf and that from the proposed model in Fig. 4.6. In fact, the Normal cdf also seems to be quite close to the empirical for errors larger in magnitude than 0.2 pu. Probability plots offer a straight forward heuristic method to assess the goodness of fit in such cases.

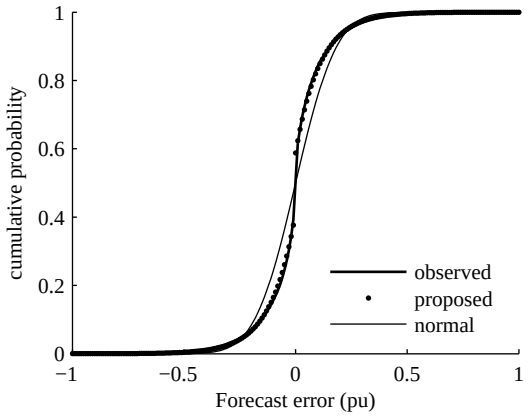

Figure 4.6: Example cdf of Observed forecast error along with the proposed model and Normal fit, using dataset 1.2004

4.3.3 Probability plots for the proposed model

Probability plots can be constructed by plotting the quantiles from a hypothesized distribution against observed quantiles. In case of an exact fit, the plotted points would lie on a line with slope = 1. Departures from this line indicate departure from the hypothesized distribution [56]. Fig. 4.7 shows the probability plots for 4 different sites for the proposed model and for the Normal approximation. The forecast period and horizon, both, are 1 hour. The departures in the tails, not noticeable in Fig. 4.6 are clearly visible. The dashed vertical lines are the limits on outliers, and the data points that are not within these limits are *suspected* outliers: the lower limit is one and a half times the interquartile range less than the first quartile, and the upper limit is one and a half times the interquartile range more than the third quartile as suggested in [57]. This rule of thumb for determining outliers works for Normal like distributions and for a Normally distributed data, less than 0.7% points would lie outside these limits.

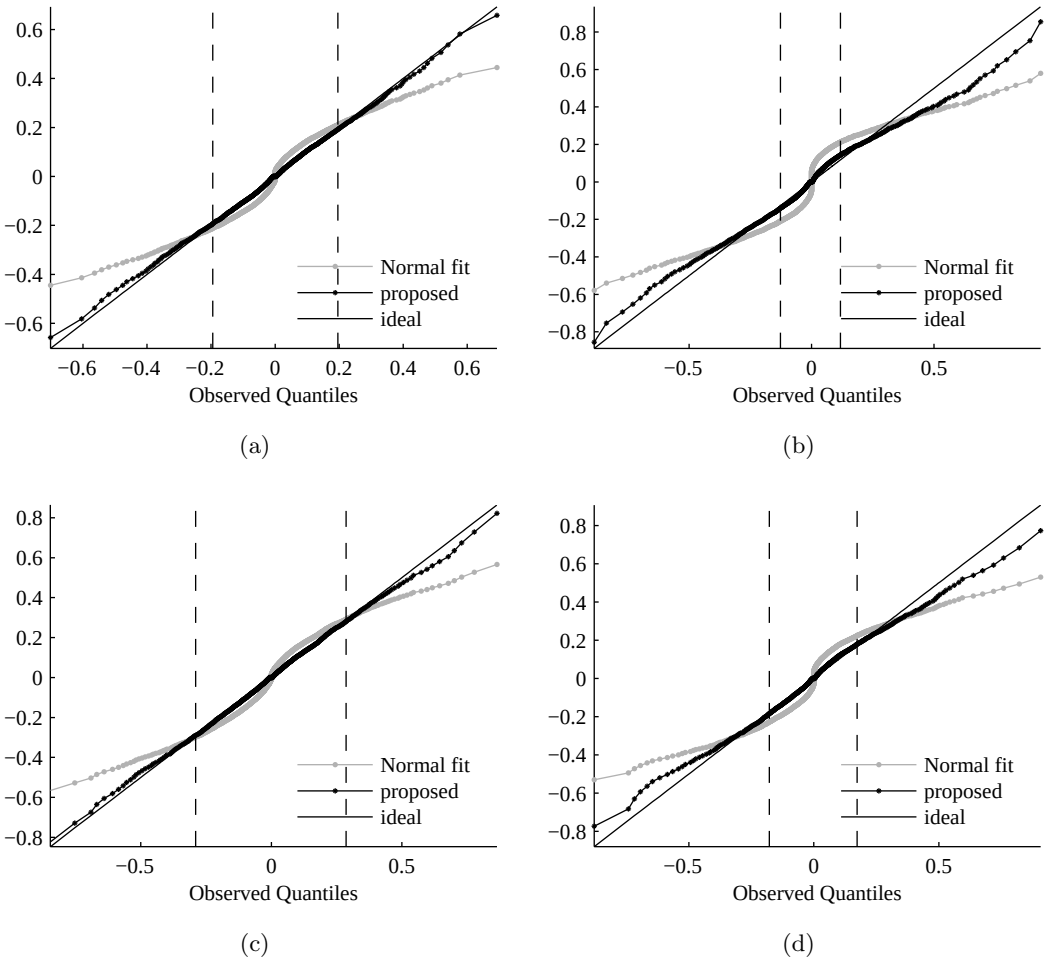

Figure 4.7: Probability plots for the Normal fit and the proposed model for the data sets (a) 1.2004, (b) 2.2004, (c) 7.2004, and (d) 8.2004. Forecast period = 1 hour, forecast horizon = 1 hour. Grey dots correspond to the Normal fit, black to the proposed model. Data points not within the dashed vertical lines are suspected outliers.

Figures 4.7(a) and 4.7(c) correspond to the data sets for which the proposed model performed good, while Figs. 4.7(b) and 4.7(d) correspond to the data sets for which the performance suffered at the extreme values (possibly outliers). It can be seen that the proposed model is a far better approximation to the actual data than the Normal approximation, and is a good approximation in general, especially within the limit on outliers.

It should be noted that while the high degree of linearity in probability plots of Fig. 4.7 justifies the use of the proposed model as an approximation to the actual distribution of the forecast error, it does not imply that the distribution of forecast error is identical to the proposed model. A claim of the latter kind can be verified only by a rigorous test like Kolmogorov-Smirnov (KS) test; however, due to the mixed nature of the proposed model, KS test cannot be used. The exact conditions and corrections for such a test are beyond the scope of this research.

4.4 Estimation of Penalties for Uninstructed Deviations

4.4.1 Uninstructed Deviation, and associated penalties

Under Midwest ISO, the generators are required to bid in the DA markets to receive capacity credit. Even if a generator decides not to commit a day ahead, it is required to stick to the dispatch instructions in real time, calculated using SCUC and SCED algorithms; or if it is self-scheduled, then stick to the schedule submitted. Injecting energy outside a tolerance band centered at the dispatch instruction is subject to penalties. Until January 05, 2009, the Tolerance Band consisted of Actual Injections that were within $\pm 10\%$ of the hourly average dispatch instructions for a given hour. It was adjusted so that it was a minimum of 5 MW and a maximum of 25 MW. It was further adjusted by adding the MW of Regulation Up and Regulation Down capacity provided by the Resource. Energy injections outside this tolerance band were known as Uninstructed Deviations (UD). Although these rules have been recently modified, they have been used in their prior form for this work to demonstrate a use of the model developed.

Until recently, wind generation was treated as intermittent and was not required to submit DA schedules. Moreover, wind resources were not dispatched like conventional resources, were paid the existing Real Time Locational Marginal Price (RTLMP) for whatever energy they injected into the grid, and were not subject to the UD penalties[1]. Fig. 4.8 shows three possible cases of deviations from the dispatch instruction: the actual injection could be lower than the lower limit of the tolerance band (negative deviation), higher than the upper limit of the tolerance band (positive deviation), or within the

[1]Wind resources are now being classified as Dispatchable Intermittent, necessarily required to participate in the RT market.

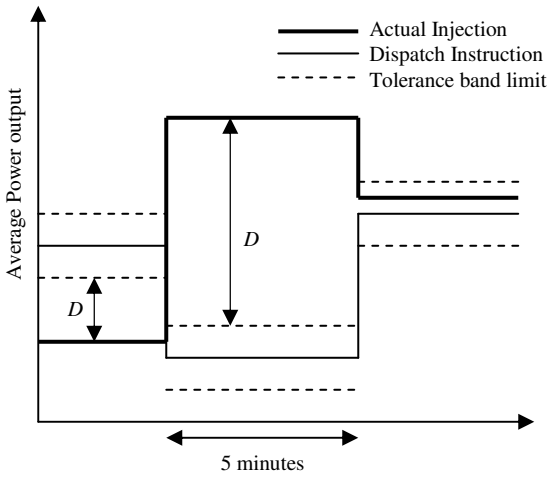

Figure 4.8: Uninstructed Deviation

tolerance band (zero deviation). Negative deviations were penalized by having to pay 40% of the price of the energy shortfall and positive deviations were penalized by being paid only 60% of the price of the excess energy injected. Therefore the loss incurred by the market participant (MP) in n hours was

$$L = 0.4 \sum_{i=1}^{n} \left[\frac{1}{12} \sum_{j=1}^{12} |D_{ij}| \times RTLMP_i \right] \tag{4.18}$$

With increased wind on system, it would be difficult to let wind generation inject arbitrary amount of energy into the grid. Energy storage is a potential solution to make wind more 'dispatchable'. However, prohibitively large amount of storage might be required to make wind dispatchable in the conventional sense. An alternative is to use the storage such that the wind farms are able to stick to their forecasted generation, so that the RTO could dispatch rest of the generation optimally.

Assume that P_{tol} is the width of the tolerance band on either side of the dispatch instruction (forecasted value in this case), and a storage capable of providing power equal to $\pm P_{ESS}$ is installed to compensate for forecast errors. If wind generation was subject to the discussed UD penalties, the forecast errors $e : |e| > P_{ESS} + P_{tol} = P'$ would be penalized according to (4.18). The term $1/12 \sum_{j=1}^{12} |D_{ij}|$ is the total Uninstructed Deviation in hour i and $RTLMP_i$ is the real time LMP for that hour. Treating these two as independent random variables, the expected hourly loss suffered by the MP could

be written as:

$$E(L) = 0.4 \times E(|D|) \times E(RTLMP) \tag{4.19}$$

Knowing the forecast error pdf, $E(|D|)$ can be calculated by an integration

$$E(|D|) = \int_{P'}^{1} e\, f(e)\, de - \int_{-1}^{-P'} e\, f(e)\, de \tag{4.20}$$

The mean value of the real time LMP could be used as the expected value.

4.4.2 A case study

Two pdfs could be used to estimate the expected deviation in (4.19): the normal pdf; and the pdf obtained from the proposed model. The actual penalties, of course, could be found only from a time step simulation. These pdfs, derived from the data of year 2004 were used to calculate the penalties for the year 2006. It was assumed that the mean value of the real time LMP is same for the two years because real time LMP data doesn't exist for year 2004.

The data used in this study is at a resolution of 10 minutes. However, the deviations are calculated every 5 minutes. Hence the resolution had to be increased by linear interpolation. The forecast period is 5 minutes and the forecast horizon is 0 minutes because the average over the last 5 minutes was used as the forecast for the current 5 minute period. Fig. 4.9 shows the variation of revenue (from 30 MW wind farms) with threshold band for the data sets indicated. The penalties have been calculated using time step simulation and also using (4.19). P' is the width of the tolerance band on either side of the dispatch instruction and is assumed to be fixed for simplicity. It can be seen that the results from the proposed model are quite close to the time step simulation even though the model has been constructed from the data corresponding to a different year. Results from the proposed model were obtained in a fairly straight forward calculation from equations (4.19) and (4.20), because of the analytical nature of the model. However, it should be kept in mind that the model is an approximation, and results from such a calculation should be used as preliminary, subject to verification from a detailed non-parametric simulation, which was done in this case study and the results were found to agree, as evident from Fig. 4.9.

Also notable is the result that the effect of the penalties is very insignificant, and is almost zero at for tolerance bands wider than 0.1 pu. As an example, the capacity factor

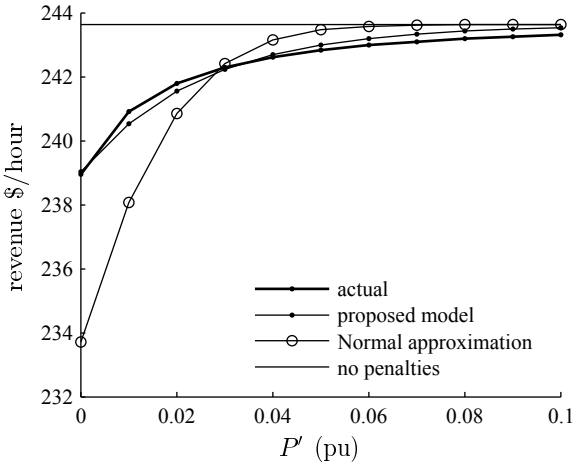

(a)

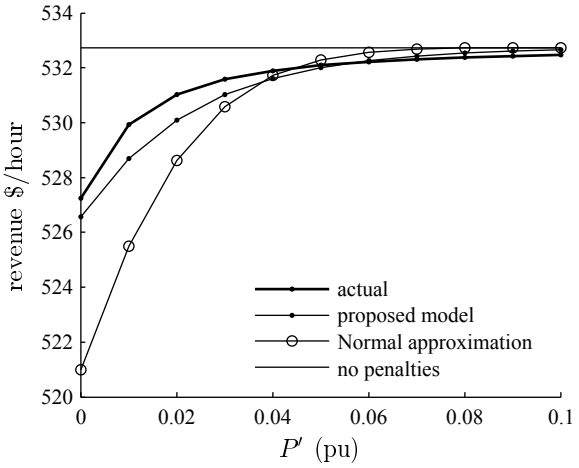

(b)

Figure 4.9: Revenue estimates from different data sets for year 2006 using data from (a) site 2, and (b) site 7

corresponding to site 7 is ∼40% which means that the dispatch instruction would be 0.4 pu on an average. Therefore the average width of the tolerance band would be 10% of 0.4 pu = 0.04 pu. Adding 0.06 pu of up and down regulation capacity using storage would make the tolerance band 0.1 pu wide, in an average sense. While the penalties would certainly be less after installing the storage, it can be seen from Fig. 4.9, that the reduction would be less than $1/hour. This is, of course, assuming that the average width of the tolerance band could be used to estimate the order of the penalties. A reduction of ∼$1/hour in penalties, upon installing 0.06 pu (1.8 MW) of storage, means that the returns would be less than $25/kW over a 5 year lifetime. The returns from storage are expressed here in terms of the up/down regulation power capability but it is implicit that the power sunk/sourced by storage would translate into some energy stored/supplied over every 5 minute period.

However, the costs of storage are of the order of hundreds of $/kW [58]. Therefore it can be concluded that storage installed for the purpose of hedging against the Uninstructed Deviations' penalties will offer little returns if wind generation is traded in RT markets only, even if it were subject to UD penalties under recent rules of the market studied. Probabilistic estimation of penalties for injecting excessive/deficient energy under the current rules/different markets is a topic for further research. It should be noted that the returns generated from storage would be higher, because of higher forecast errors, for the markets in which wind generation would be required to submit schedule several hours ahead. Also, the value of storage would be enhanced if it was applied at a system level, as opposed to the level of a single wind farm, since errors from multiple resources would cancel each other, leading to a smaller error to installed capacity ratio. However, it is a policy issue to allow multiple wind resources to share a storage facility, and to work out the details of such an arrangement. It must also be noted that hedging against UD penalties is only one of the value propositions offered by energy storage. Other gains that could be realized using storage are deferred investment in transmission lines, energy trading, and ancillary services.

4.5 Geographical dispersion and the distribution of forecast error

Assuming that the forecast errors from geographically dispersed wind farms are independent, we would expect the sum of forecast errors, or the forecast error for total wind power, to have a Normal distribution from the Central Limit Theorem (CLT). The distribution of error from 20 different sites marked in Fig. 4.4 was examined on an individual and net basis. It was found earlier that the individual errors were far from being normally distributed (Fig. 4.7). Fig. 4.10 shows the Normal probability plots for the net forecast error and the error from a single site for year 2004. Departure from the straight line indicates departure from normality. The outliers are highlighted similar to Fig. 4.7.

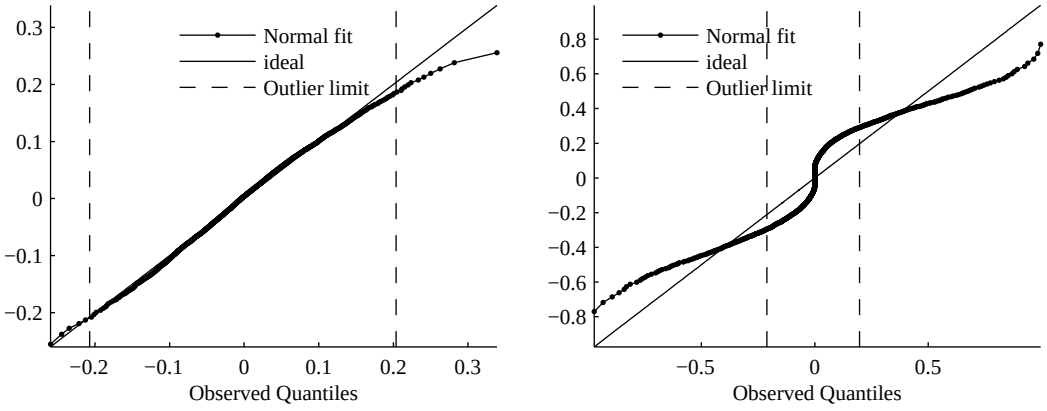

Figure 4.10: Normal Probability plots for (a) total forecast error from 20 sites for year 2004, and (b) for forecast error for data set 2.2004. Forecast period = 1 hour, forecast horizon = 3 hours. Data points outside the dashed lines are suspected outliers.

While none of the data, net or individual, is normally distributed, the net error is much closer to being normally distributed than the individual error: the net error coincides with the straight line most of the time while the individual error almost never coincides with the straight line. Also, the total forecast error is even closer to being Normally distributed if the outliers are ignored. As the number of sites increases, the

linearity should increase as expected from CLT and Fig. 4.10 serves as a testimony to that.

Using the Normal model is certainly convenient because if load forecast error also follows a Normal distribution, which is commonly assumed [8, 9, 47, 48, 50], then the convolution in (4.4) is greatly simplified. In fact, in that case the total system error also follows a Normal distribution with mean and variance equal to the sum of means and variances of wind and load forecast errors.

The assumption that wind power forecast error is normally distributed should work perfectly well on a system level where the power outputs, and hence forecast errors, from different farms could be treated as independent. It is noteworthy that this assumption, although examined here for Persistence forecasts, is independent of forecasting methodology and forecast horizons. Also, forecast errors don't have to be pairwise independent for every given pair: as long as forecast errors between several areas are independent, the normal assumption would hold. Of course, sufficient transmission must exist such that power can freely flow in a wide area, allowing the forecast errors to be summed up.

Concluding remarks

It has been shown that the wind power forecast error resulting from the Persistence methodology has a point probability at 0 pu, and therefore, it cannot be treated like a continuously distributed random variable. A statistical distribution model for the forecast errors associated with the Persistence method for a single wind farm has been developed which recognizes the discrete and continuous character of the forecast error. The model has been used to calculate the penalties for the Uninstructed Deviations in a North American market, and the results indicate that energy storage at the level of a wind farm might not be an economically feasible option to hedge against the aforementioned penalties. However, storage can generate profit by energy trading, by deferring investment in transmission lines, and by offering services in the ancillary services market. It has also been shown that the statistical distribution of net error from geographically dispersed sites approaches the Normal distribution, as expected from the CLT.

Chapter 5

An optimal strategy to dispatch storage in Real Time markets

Transmission constraints cause the locational variability in the energy market LMPs. Inability to import and export energy can cause the LMPs to become unusually high or low, especially in the RT market. Although the levelized cost of generation from wind is lower than peaking combustion turbines [35], and wind is expected to reduce the LMPs in an average sense [30], wind could easily cause perturbations in the prices in absence of adequate transmission:

- Negative LMPs imply generation in excess of the demand at a location. The Federal government of the U.S. provides renewable energy production credit [60] to support higher contribution of renewables to meet the energy demand. Because of these production credits, wind resources could continue to produce (and earn revenue) even when the prices are negative, exacerbating the problem of excess generation.

- In an opposite case, unexpected calm periods in wind can drive the prices up to the extent that LMPs reflect the value of lost load (VOLL).

However, if there is energy storage on the system, the excess power could be absorbed when generation exceeds demand and discharged later, when the generation falls short. There are several benefits to this approach — wind resources continue to generate and

earn revenue critical for their feasibility, the system doesn't need transmission upgrade, and the stored energy that was purchased at very low (even negative) prices could be sold later when the prices are high, in addition to stabilizing the prices.

This chapter presents a strategy to dispatch energy storage in RT markets such that the revenue is maximized while the number of cycles stays low. Although the procedure is applicable to all storage technologies, the parameters assumed are closest to battery energy storage.

5.1 Day Ahead v. Real Time

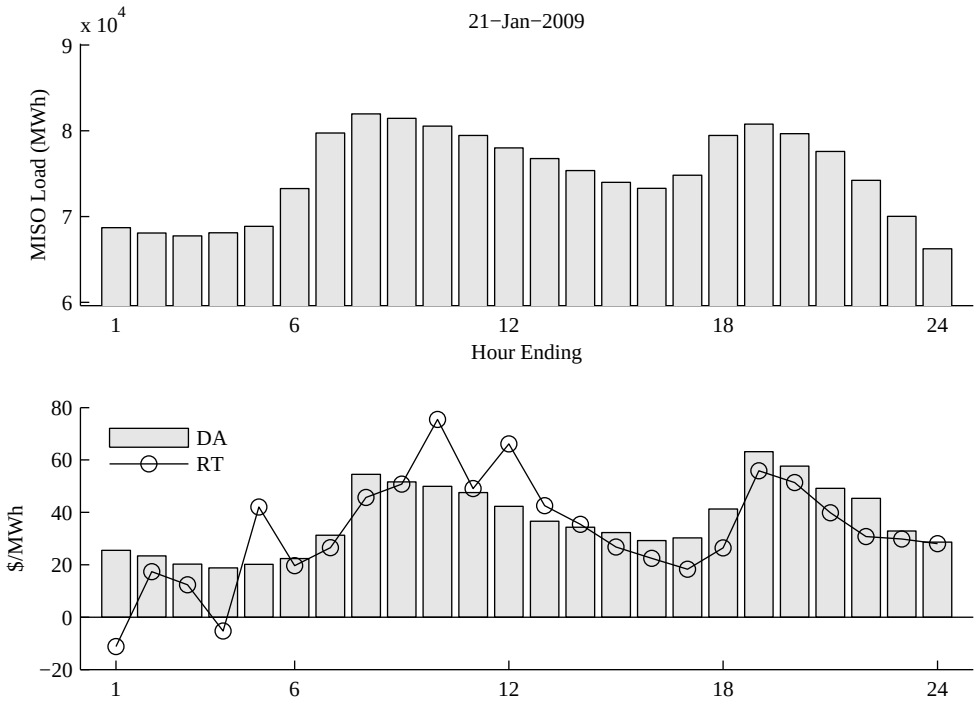

Figure 5.1: The MISO systemwide load and DA, RT prices at MINN.HUB on January 21, 2009

Fig. 5.1 shows the system wide load for Midwest ISO on January 21, 2009, and the DA and RT prices at the MINN.HUB pricing node for the same day. It can be seen that the DA prices follow the load to a large extent while the RT prices vary more randomly,

over a larger range.

Although the RT prices could follow the load for other days, and Fig. 5.1 only illustrates a specific day, the fact that the relationship between prices and load is more predictable for DA market is easily seen from the correlation coefficients in Table 5.1.

Market	Correlation coefficient
Day Ahead	0.79274
Real Time	0.53942

Table 5.1: Correlation coefficients of the prices at MINN.HUB with the system wide load for the year 2009

Not only the RT prices are less predictable, they are spread over a much larger range as seen from the boxplots in Fig. 5.2. The fact that Real Time prices could easily become negative implies that storage could be very profitable in the RT market.

Therefore, considering the relatively high randomness and wide range of RT prices, and the fact that storage can act fast enough, it makes sense most to trade storage in the RT market.

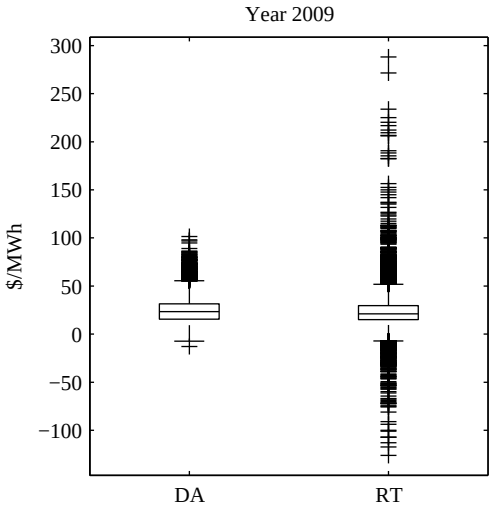

Figure 5.2: Boxplots of the DA and RT prices at the MINN.HUB for year 2009

5.2 A method to dispatch storage in Real Time markets

The RTLMPs are a product of innumerable factors and are impossible to model analytically, similar to stock prices. However, they can always be treated like random variables to use them in a mathematical framework. Let the RTLMPs be the instances of a random variable X that has an unknown distribution. By probability integral transform [61], the cumulative distribution function of X is uniformly distributed in $[0, 1]$

$$F(X) \sim \text{Unif}[0, 1] \tag{5.1}$$

$$\Rightarrow \underbrace{2 \times \left(F(X) - \frac{1}{2} \right)}_{:=U(X)} \sim \text{Unif}[-1, 1] \tag{5.2}$$

$U(X)$ can serve as as the dispatch instruction because,

1. $U(x) = 0$ when $x = \text{median}(X)$. Therefore $U(X)$ is such that the storage is allowed to charge when the prices are below the median price and is allowed to discharge when the prices are above the median price.

2. $E(U(X)) = 0$. Therefore the battery is allowed to discharge only as much as it is allowed to charge, in an average sense. Please note that $U(X)$ as defined in (5.2) can be easily adjusted to account for sub-unity round trip efficiency.

3. Most importantly, $U(X)$ is directly related to the "extremeness" of the RTLMP, X. $U(X)$ increases in magnitude as X moves away from the median price. Therefore extreme prices imply high charging/discharging rates, which is consistent with how one would want to operate the battery.

However, $U(X)$ approaches the bounds of its range only as the prices approach their maximum and minimum but it might be desirable to charge/discharge the storage at its maximum rate even when the prices are not at their extremes. To rectify this potential problem, $U(X)$ could be multiplied by a constant $k > 1$, and then saturated at ± 1. Note that the resultant function will still have a uniform distribution (although mixed,

no longer continuous) and will retain the properties 1 through 3 described above. The resulting function could be written as

$$V(X,k) = \begin{cases} +1 & kU(X) \geq 1 \\ kU(X) & kU(X) \in (-1,+1) \\ -1 & kU(X) \leq -1 \end{cases} \tag{5.3}$$

Further, $F(X)$ is not known as a function of X and could only be estimated from the existing data. The problem with this approach is that because of the relatively nascent, and possibly non-stationary character of the markets, the cumulative distribution function (cdf) $F(X)$ estimated from the existing data might not be valid. For example, Fig. 5.3 shows the cdfs of RTLMPs for the years 2009 and 2010. While the two functions might seem very close when viewed over the entire range of RTLMPs, upon close inspection significant departures are noted that are clearly shown in Fig. 5.3. Consequently the $V(X,k)$ derived from existing data would be suboptimal. Therefore a deadband μ must be provided in the vicinity of the median price such that the charging/discharging occurs only when the prices are sufficiently far from the median. The

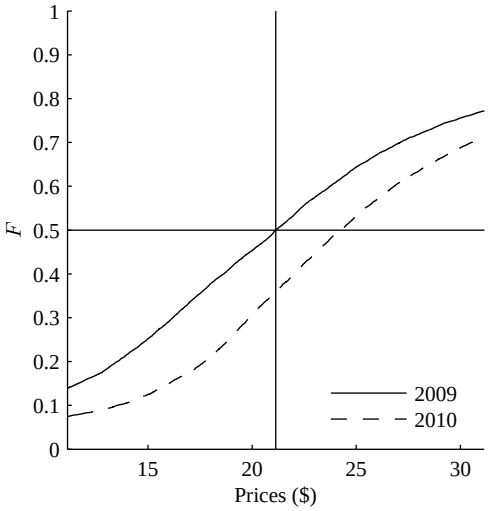

Figure 5.3: cdfs of the RTLMPs for the years 2009 and 2010

resulting dispatch function could be written as

$$r(X,k,\mu) = \begin{cases} 0 & |V(X,k)| \leq \mu \\ V(X,k) & |V(X,k)| > \mu \end{cases} \tag{5.4}$$

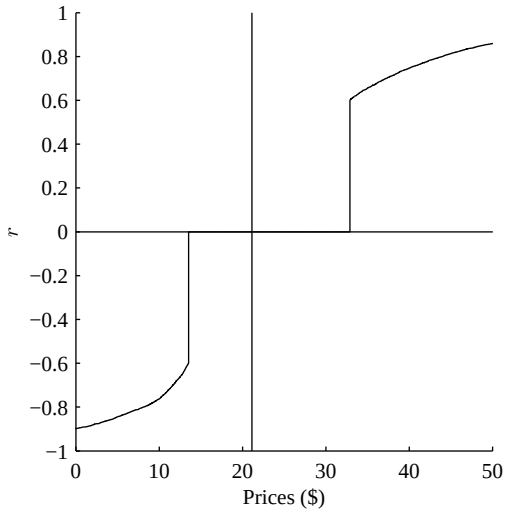

Figure 5.4: Discharge rate derived from RTLMP data for 2009

A plot of $r(X,k,\mu)$ can be seen in Fig. 5.4 for some value of (k,μ), when the cdf $F(X)$ was derived from the RTLMP data for the year 2009. If $U(X)$ derived from 2009 RTLMPs was used for dispatch in the year 2010, the storage would be discharging below the 2010 median price (please see Fig. 5.3) but this problem is alleviated using the deadband approach (Fig. 5.4).

5.3 Optimizing the parameters

The dispatch function $r(X,k,\mu)$ depends upon k,μ. In addition, energy capacity per unit power rating ($:= E$) is also a parameter for the storage. Because the actual charging/discharging rate would be influenced not only by the function r, but also by the State of Charge (SOC) of the storage, E should also be included in the final charging/discharging rate.

$$|r_E(X,k,\mu)| \leq |r_\infty(X,k,\mu)| \tag{5.5}$$

The actual charging/discharging rate could be equal to dispatch function only in case of unlimited energy capacity. The revenue could now be defined as

$$P = \sum_{i=1}^{n} r_E(X, k, \mu)[i]X[i] \tag{5.6}$$

where the index i represents the i^{th} hour. The storage usage could be written as

$$L = \sum_{i=1}^{n} |r_E(X, k, \mu)[i]| \tag{5.7}$$

The optimal set of parameters would maximize P while keeping L low. Therefore the ratio P/L is of interest, at acceptable values of P. In this work, $r_E(X, k, \mu)$ derived from the RTLMP data of 2009 was used to simulate the storage dispatch for the prices of the years 2009 and 2010. The range of parameters is shown in Table 5.2. It can be seen that the values of the energy capacity E are closest to battery storage (few MWh per MW).

μ	$\{0, 0.1, \ldots, 0.6\}$
k	$\{1, 3, 5\}$
E	$\{1, 3, 5\}$

Table 5.2: Range of parameters

5.3.1 Results

Fig. 5.5 shows the revenue against battery usage for the sets of parameters in table 5.2. $r(X)$ was estimated from RTLMPs of the year 2009 and then used to dispatch the battery in the year 2009 ('$\times$' markers in the figure) and the year 2010 ('$\bullet$' markers). The grey line segments connect the results for the years 2009 and 2010 with the same set of parameters k, μ, E and it can be seen that the estimates from training ($F(X)$ from 2009 applied to 2009) and testing ($F(X)$ from 2009 applied to 2010) are not too far off.

It is also seen that that varying the parameters shifts the results over a wide range of revenue, usage, and their ratio. The 6 best performing sets of parameters (sorted by the ratio of revenue to usage) are tabulated in table 5.3. Note that some cases

were degenerate ($\{P, L\} = \{0, 0\}$), for example $\mu = 0.6, E = 1$. This is because the starting SOC was 0.5 and any dispatch command would have resulted in SOC violating its bounds.

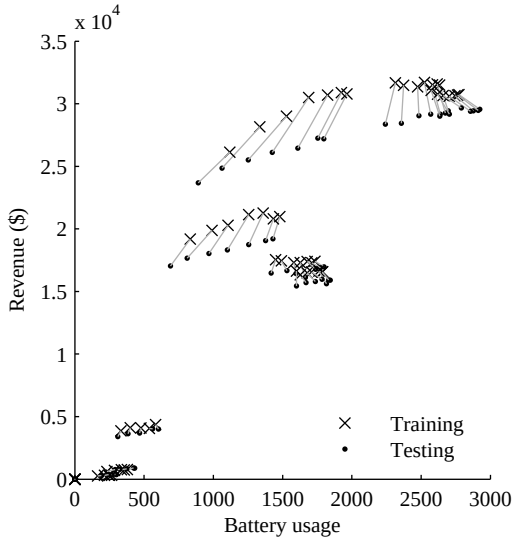

Figure 5.5: Revenue against battery usage for years 2009 (training) and 2010 (testing) using $r(X)$ derived from 2009 data.

μ	k	E (MWh/MW)	Usage L	Revenue P (\$)	P/L
0.6	1	5	891.56	23676.08	26.56
0.6	1	3	690.09	17034.52	24.68
0.5	1	5	1063.27	24856.93	23.38
0.5	1	3	810.76	17667.84	21.79
0.4	1	5	1251.98	25513.88	20.38
0.4	1	3	968.50	18031.99	18.62

Table 5.3: Best performing sets of parameters

5.3.2 Discussion

It is easily seen that the value of the multiplier k is equal to 1 for the best cases of Table 5.3: this means that extreme charging/discharging rates for relatively moderate

prices are not preferable. Furthermore, the ratio P/L increases steadily with the deadband μ, meaning operation close to the median price is not favorable. Combined, it can be concluded that operating the energy storage conservatively, and only at the relatively extreme prices, is optimal for maximizing the revenue per unit usage.

However, it might be desirable to earn more revenue at the cost of somewhat lower P/L to expedite the returns. The degree to which P/L could be sacrificed in favor of higher revenue would depend upon the investment and the lifetime of the storage technology.

It is also seen that a higher energy capacity is better from a revenue (trivial) and a revenue/usage perspective, for the same set of $\{k, \mu\}$.

Concluding remarks

A price sensitive strategy to dispatch energy storage in the RT markets has been proposed, and the parameters of the resource (E), and the resource offer (k, μ) have been optimized.

Note: Part of this chapter is reproduced from the author's publication [62] and the copyright holder is The Society for Modeling and Simulation International.

Chapter 6

Commercial location strategy

It was explained in the Introduction that the financially optimal location would also be optimal from a transmission system standpoint. This chapter presents an analysis towards finding such location based on the returns from economic dispatch. A strategy for economic dispatch was described in the previous chapter. The strategy used in this chapter was developed by Xcel Energy. The strategy in the last chapter dispatched energy storage in the RT market only while this strategy dispatches the battery in both, DA and RT, markets. The strategy is described first, followed by the commercial location analysis.

6.1 Economic dispatch

This strategy seeks to maximize the revenue generated from energy trading by offering the battery in the MISO DA and RT markets. The brief description here is based on Xcel Energy's presentation titled "W2B Preliminary Storage Analysis" dated 05/27/2009. The features and configurable parameters include, but are not limited to:

- Day ahead (DA) must run (MR) hours selected on the basis of past day's DALMPs.
- Hours not included under MR fall under Economic Dispatch (ED):
  - DA ED charge/discharge rates decided on the basis of time of the day and deviation from the mean DALMP.

  - RT ED charge/discharge rates decided on the basis of time of the day and deviation from the mean DALMP.

- Also takes the SOC into account.
- Charge/discharge rates variable in $\{-100\%, -50\%, -25\%, 0\%, 25\%, 50\%, 100\%\}$
- Further optimization using Oracle Crystal Ball.

A crude version of the above algorithm was implemented in MATLAB that does not account for the intra-hour movement of RTLMPs and does not optimize the configurable parameters. Furthermore, this implementation does not differentiate between weekdays and weekends. The results from this program were consistent with an earlier version of Xcel Energy's spreadsheet program with the same limitations as this version. This implementation in its current form was used to simulate the economic dispatch for location analysis. Clearly, this version underestimates the revenue. However, because the flaws are uniform across all nodes, the results of location analysis presented in the next section should still hold.

6.2 Commercial location

This analysis seeks to find the best location to place the battery (within NSP) to maximize the revenue from economic dispatch. To this end, the DA and RT LMP data at 213 nodes under the NSP territory was analyzed. The data was taken from MISO's website and corresponds to the period of 10/1/2010 – 12/31/2010 (92 days). Only nodes with a minimum of 30 days of data were considered.

The natural methodology would be to apply the strategy of section 6.1 to all the nodes. However, this would not provide any insight into the problem. An alternative is to screen the nodes on the basis of some explanatory criteria and study the effect of these criteria on the revenue at the screened nodes.

It is intuitively clear that a higher spread in the prices would mean higher revenue for the battery. Variance (standard deviation) is a commonly used measure of spread. Range is another such measure. Although a monotonic trend was found between the

90% range[1] and the variance, the trend was not strong enough to justify using only one of the two measures.

Another somewhat related measure is the mean absolute error of the prices about the median price. While impossible to realize in practice, the absolute error about the median price of a market is the upper bound on the revenue earned by the battery in that market. Considering that the strategy of Section 6.1 offers the battery in both DA and RT markets, following criteria were used to screen the nodes:

1. Variance of the DA and RT LMPs.
2. 90% range of the DA and RT LMPs.
3. Absolute error in the DA and RT LMPs about their median values.

For each of the above criteria, 10 top and bottom nodes were identified. While identifying the bottom nodes is not of direct interest to this analysis, it is expected to validate the choice of criteria itself, and to help identify the most influential criteria. Because of significant overlap, the list of identified nodes is much shorter than 120 nodes; the nodes are listed in Table 6.1.

Economic dispatch of the battery using the strategy of Section 6.1 was simulated at the all the nodes for the period of 10/1/2010 – 12/31/2010. The mean daily revenue across all nodes was \$120.06 with a standard deviation of \$23.10. The median revenue was \$117.99. The results are plotted in Figs. 6.1 and 6.2.

[1] 90% range is the range after discarding 5% of the highest and lowest values. Discarding the extreme values tends to improve the robustness of the measure.

(a) List of top nodes

Node name	Node type
NSP.VELVAVELV	Gennode
NSP.WHEATO5	Gennode
NSP.WHEATO6	Gennode
NSP.WHEATO3	Gennode
NSP.WHEATO4	Gennode
NSP.WHEATO2	Gennode
NSP.WHEATO1	Gennode
NSP.CHPFAL1	Gennode
NSP.CHPFAL2	Gennode
NSP.CHPFAL4	Gennode
NSP.BE	Loadzone
NSP.BELW_1.AZ	Hub
NSP.HCPD.MAD	Loadzone
NSP.UPLS_3.AZ	Hub
NSP.HCPD.LKCR	Loadzone
NSP.HATFIHAT1	Gennode
NSP.MENOMOA	Gennode
NSP.EWINGTON1	Gennode
NSP.CISCO1	Gennode
NSP.GARWIN1	Gennode
NSP.MOWERCO1	Gennode
NSP.RAPIDA1	Gennode
NSP.GDMEADOW	Gennode

(b) List of bottom nodes

Node name	Node type
NSP.OTP	Loadzone
NSP.OTPW_1.AZ	Hub
NSP.CMMPA.GF	Loadzone
NSP.GFLS	Loadzone
NSP.UPLS_2.AZ	Hub
NSP.FIBROMIN1	Gennode
NSP.BUFFR_TR1	Gennode
NSP.BUFFR_TR2	Gennode
NSP.OAKLKE_IBR	Gennode
NSP.NIPS.YANKE	Gennode
NSP.SHERCO2	Gennode
NSP.SHERC3	Gennode
NSP.SMP.S3	Gennode
NSP.SHERCO1	Gennode
NSP.WESTSID1	Gennode
NSP.GRANCT1	Gennode
NSP.ADAMSWD1	Gennode
NSP.DANIELSN1	Gennode
NSP.RWF__1_QS	Gennode
NSP.RWF__2	Gennode
NSP.HIBRDG9_1	Gennode
NSP.HIBRDG9_2	Gennode
NSP.CC.HIBRDG1	Gennode
NSP.CC.HIBRDG2	Gennode
NSP.HIBRDG.7	Gennode
NSP.HIBRDG.8	Gennode
NSP.SPGSPG1	Gennode
NSP.YANKE_TR1	Gennode

Table 6.1: The list of (a) top and (b) bottom nodes identified for detailed economic dispatch analysis.

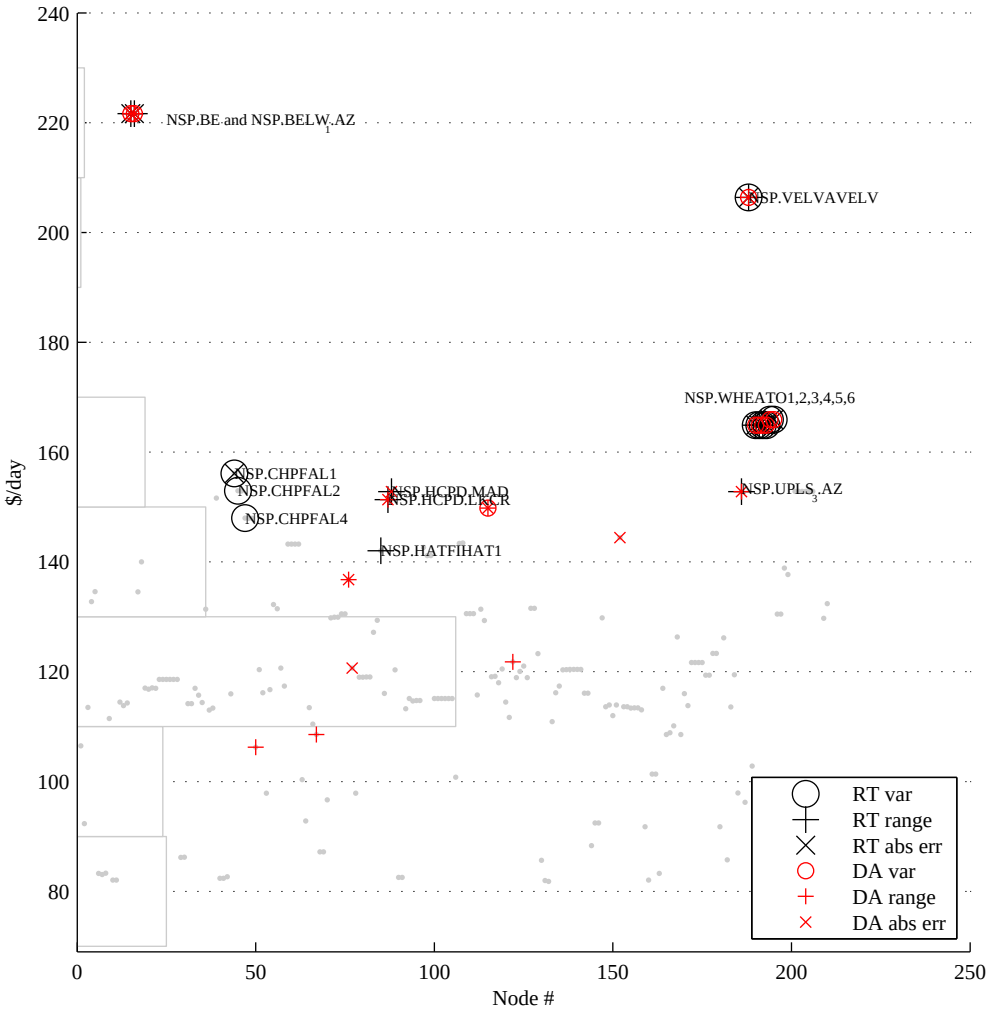

Figure 6.1: Revenue at each of the 213 NSP nodes plotted against node number (chosen alphabetically). Each grey dot represents the average daily revenue at a NSP node; the grey bar chart is the histogram of the average daily revenue across all nodes. The nodes at which the revenue was expected to be high are represented by ◯, ┼, × and ○, +, ×. The color black represents the nodes chosen on the basis of the statistics of the RT prices and the color red represents the nodes chosen on the basis of the statistics of the DA prices. E.g. the node NSP.UPLS_3.AZ has been chosen on the basis of the range of the DA (+) and RT (┼) prices and on the basis of the absolute error (about the median) in the DA prices (×). It is seen that the variance, range and absolute error of the RT prices, and the variance of the DA prices are good predictors of the total revenue — they succeed in exhaustively identifying the nodes with revenue greater than $160/day without identifying any node with revenue less than $140/day. On the other hand, the prediction performance of the range and absolute error of the DA prices is poor and they identify some nodes with revenue close to or lower than the mean revenue.

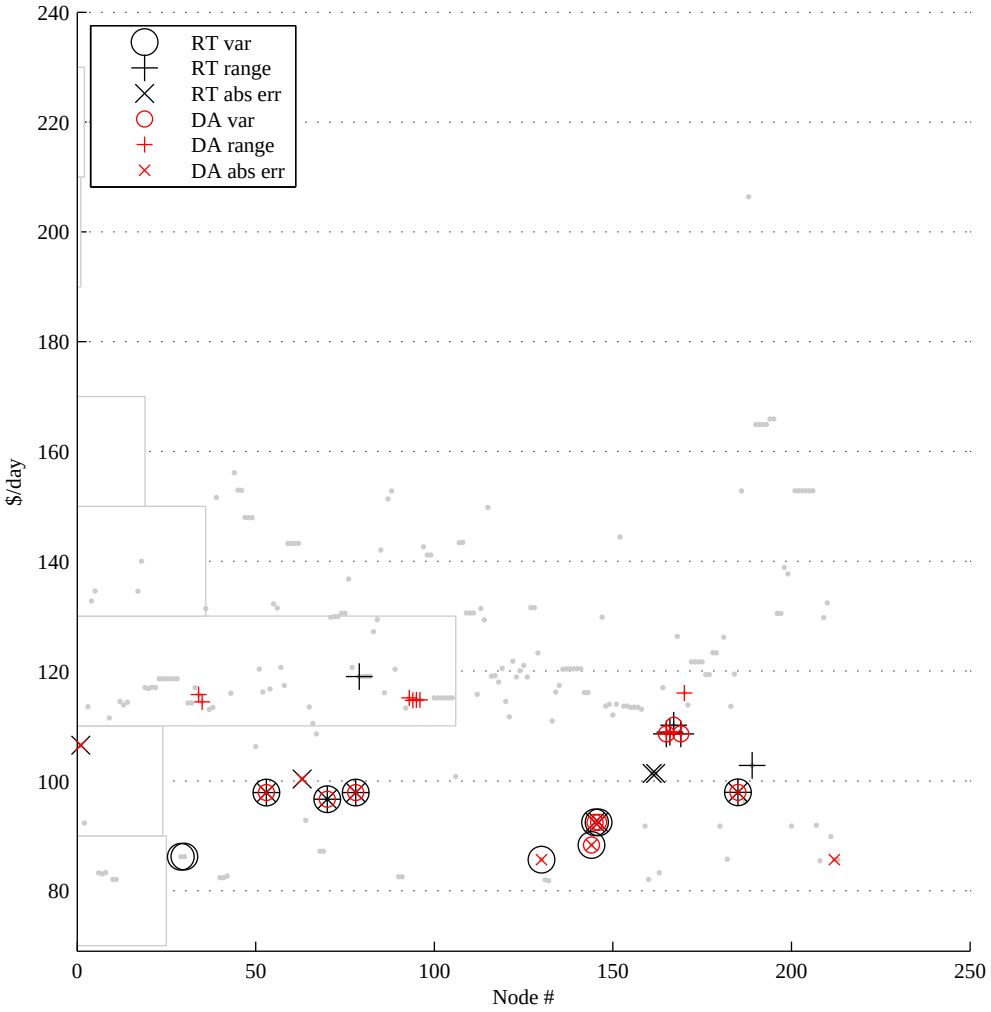

Figure 6.2: In this plot the nodes expected to have the lowest revenue have been marked. None of the criteria is able to indentify the nodes with lowest revenues, but all criteria successfully avoid identifying any node with revenue higher than the mean revenue. Most of the nodes with higher revenues among the identified nodes are predicted by the DA range, establishing it as a poor predictor.

Concluding remarks

From the results of Fig. 6.1, the best nodes for locating the battery are NSP.BE, NSP.BELW_1.AZ and NSP.VELVAVELV. The best predictors of the revenue from the

strategy considered are the variance of DA and RT LMPs, and the range and mean absolute error (about the median) of RTLMPs.

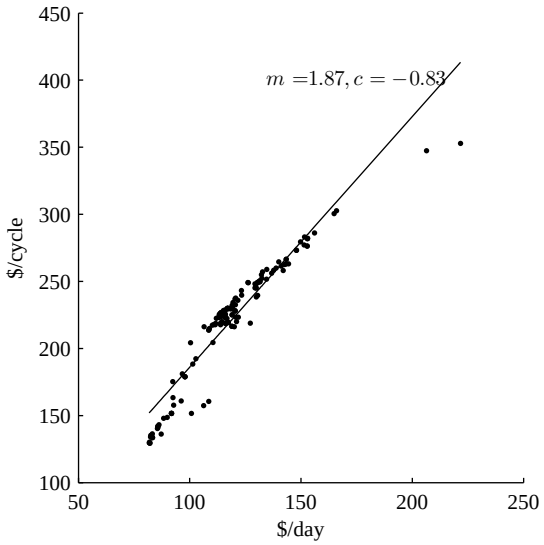

Figure 6.3: Per cycle revenue plotted against per day revenue.

Fig. 6.3 shows the revenue per cycle plotted against the revenue per day, and the relationship is certainly monotonic. Therefore the nodes with high revenue per day will also have high revenue per cycle, meaning highest return over the lifetime of the battery. Furthermore, the relationship in the Fig. 6.3 is not linear and the nodes with the highest revenue fall on the right of the best fit line: these nodes will exhaust higher number of cycles per day, with a higher revenue per cycle. This implies not only the highest, but also the fastest return on investment at the selected nodes (NSP.BE, NSP.BELW_1.AZ (overlapping) and NSP.VELVAVELV).

Without adjusting for inflation, the best case offers returns at $221.66/day and $352.87/cycle. For a cycle life of 4,500 cycles this translates to a lifetime return of about $1,600,000 realized over almost 20 years. According to [32], the lifetime of the battery is 4,500 cycles and 15 years. Therefore other functions (chapters 3, 7) need to be integrated with energy trading to realize the returns faster, especially during the float period.

Chapter 7

Value in the Ancillary Services Market (ASM)

7.1 Data, resource offer, and key assumptions

7.1.1 Data used

The time period considered in this study is 8/18/2011 – 9/17/2011. The following prices available on the Midwest ISO (MISO) website are used for this study:

- SERREGMCP (referred to as MCP for the rest of this document).
- DEMREGMCP (found to be equal to the above for the duration considered).
- GENREGMCP (found to be equal to the above for the duration considered).
- Real Time LMP.

All of the above are systemwide prices. The MCPs used are the Day Ahead MCPs and the scope of this study is limited to DA Regulation Market (ASM). For the purpose of the presented analysis, the battery is assumed to be ideal:

- The battery can act infinitely fast.
- The efficiency is 100%: Since the revenue earned by the battery does not depend

upon the actual MWh sourced/sunk (Section 7.2), the revenue would not be affected by efficiency. However, the revenue/usage in Fig. 7.4 and Table 7.2 would be slightly lower.

7.1.2 Price sensitive offer

Under the framework of MISO ASM, Energy Storage could only be offered as a Regulating Reserve. See Exhibit 4-9: Resource Eligibility Summary for Provision of Operating Reserve in [27]. The prices for Stored Energy resources offered towards Regulation Reserve requirement in the DA ASM market are called SERREGMCP and would be referred to as MCP hereafter.

Fig. 7.1(a) shows the histogram of MCPs for the duration of this study. It is seen that the highest prices have the lowest probability of occurrence. MISO accepts up to ten MW-price pairs for the resource offer [27]. It makes most sense to offer the entire MW capability of the resource when the prices are high and to be more conservative at lower prices. This strategy is expected to balance the revenue against the battery usage (and hence lifetime).

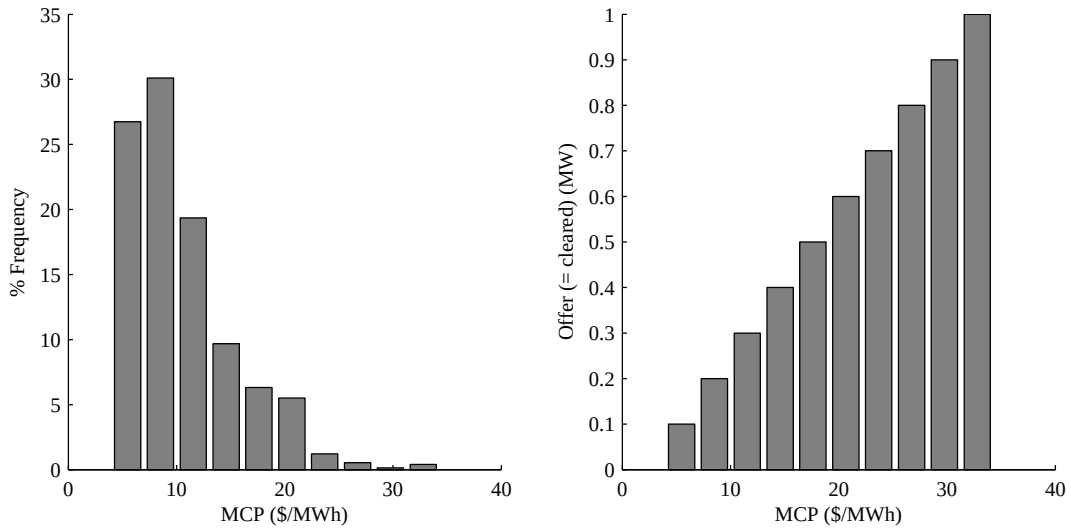

(a) Histogram of MCP

(b) Resource offer

Figure 7.1: Prices and price sensitive offer

For this work, a resource offer linearly dependent upon the price has been used: the offer goes up by 0.1 MW when prices increase by 10% of their range. Fig. 7.1(b) shows the price sensitive resource offer. Other non-linear offers similar to [62] are possible.

7.1.3 Key assumptions

In addition to the assumptions about the battery, following additional assumptions are made:

1. **The offer is always accepted**: It is not possible to simulate the precise market behavior without modeling the entire system using a tool like PROMOD. However, if the MCP can indeed be considered a measure of regulation resources' availability on the system, then an offer based on historical prices should not be far off from what would actually clear.

   The resource offer, as seen from Fig. 7.1, is seldom asking for extreme prices; and the offer is generally close to the median price. Furthermore, in absence of the entire system model, historical prices and their distribution should be the best indicators of what could be considered a fair offer.

2. **The regulation requirement is random**: The MCP is set by designated regulation requirement and resource offers, not by the actual regulation requirement because that would be impossible to predict; if at all it was possible to predict the actual regulation requirement, there wouldn't be any need for a regulation market[1].

   The actual regulation requirement would be the energy deficit or excess that wasn't met by the DA and RT markets. This requirement is unpredictable and could be positive or negative. Under the assumption that it is indeed random and uncorrelated with LMPs and MCPs, it has been modeled as a zero mean Normally distributed random variable with standard deviation chosen such that it lies within $\pm$400 MW 99% of the time. The number 400 (MW) was advised by domain expert, Rao Konidena (MISO).

[1]Here 'regulation requirement' or 'actual regulation requirement' implies the requirement imposed on the regulation reserves in real time. The amount of regulation reserves that the system should carry is called 'designated regulation requirement'.

7.2 Mehtodology

Under the above assumptions, following methodology is adopted to establish the value of battery in ASM:

1. Generate random time series for the actual regulation requirement. The resolution is one hour but it is possible to make it finer.

2. The setpoint for the battery would be based on the cleared MWs and the actual regulation requirement. For instance, if the actual regulation requirement is +300 MWs and the battery is cleared for 0.5 MW, the setpoint would be +0.375 MW.

$$\text{SETPOINT} = \text{DA\_ASM\_VOL} \times \frac{\text{REG\_REQ}}{\min(400, |\text{REG\_REQ}|)} \tag{7.1}$$

   Here SETPOINT is the MW setpoint, DA_ASM_VOL is the hourly DA cleared regulation volume and REG_REQ is the actual regulation requirement on the system.

3. However, if the battery is nearing the limits of its State of Charge (SOC), the SETPOINT is forced to 0 and the battery is charged/discharged at its maximum capability. The Asset Owner (AO) incurs the costs in proportion to the volume charged/discharged and the RTLMP.

4. The revenue is then calculated as [34]

$$\begin{aligned}\text{REVENUE} = \sum_{\text{hours}} (&\text{DA\_ASM\_VOL}_{\text{hour}} \times \text{DA\_REG\_MCP}_{\text{hour}} \\ &- \text{RT\_VOL}_{\text{hour}} \times \text{RT\_LMP}_{\text{hour}})\end{aligned} \tag{7.2}$$

   Here DA_REG_MCP is the MCP, RT_VOL is the MWh *drawn* from the system in real time and RT_LMP is the Real Time LMP.

5. Becuase it is not possible to count charging/discharging cycles in this application, the cycles are substituted by "usage" which is defined as the absolute integral of battery MWs.

$$\text{USAGE} = \sum_{\text{hours}} (|\text{SETPOINT}_{\text{hour}}| + |\text{RT\_VOL}_{\text{hour}}|) \tag{7.3}$$

Fig. 7.2 illustrates the procedure above. It is seen in the figure that cleared volume follows the MCP closely (although in discrete steps) while the actual MW setpoint is also dependent upon the regulation requirement. The actual regulation requirement is independent of the MCP and is random.

It is also seen that the battery needs to charge during HE233 because of low SOC and the revenue falls because of RTLMP paid during that hour. If the maximum volume offered is kept below the physical MW capacity of the battery by introducing a scaling factor $k < 1$, it might be possible to minimize the exposure of the battery to RT market. This could also be thought as a lower slope of the offer-MW plot in Fig. 7.1(b). Such a constant scaling factor would mean lower revenue, but also lower usage. Whether it is beneficial or not is explored in the next section.

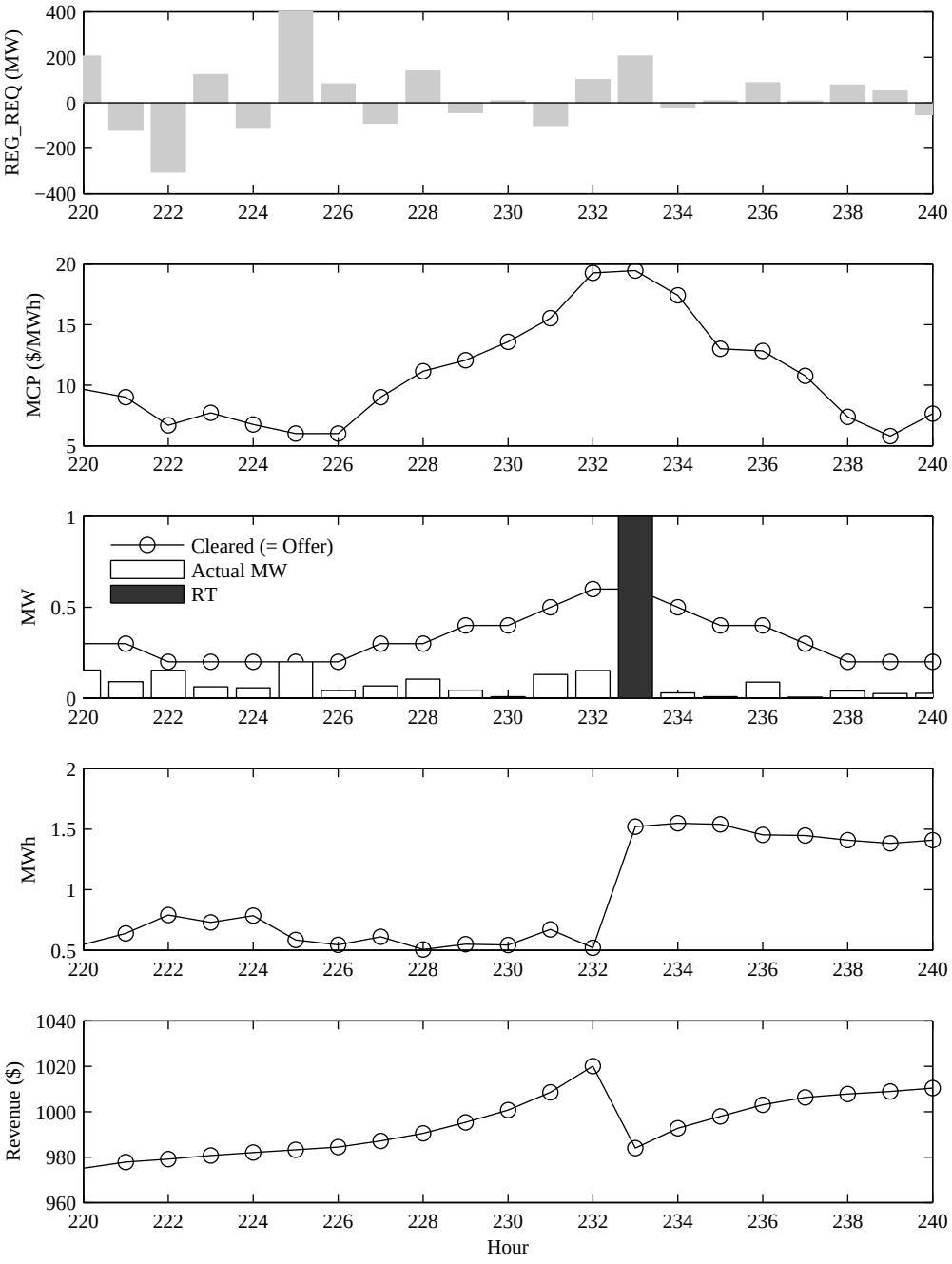

Figure 7.2: Storage operation from top — The actual regulation requirement; MCP; The cleared volume, actual MW setpoint in accordance with (7.1) and RT volume; MWh; and bottom, revenue. Energy storage operates normally during all hours except HE233 during which emergency charging is necessary.

7.3 Monte Carlo simulation

Monte Carlo method involves simulation with random input for a sufficiently large number of times to obtain the distribution of the output. Following procedure was adopted:

1. Set scaling factor to 100%.
2. Generate regulation requirement (a random sequence).
3. Follow the steps in the last section to compute the revenue and usage and save their values.
4. Repeat the above three steps such that the simulation is run 100,000 times.
5. Repeat the above four steps at scaling factors 75%, 50% and 25%.

The results are presented in Figs. 7.3(a) and 7.3(b).

As expected, when the entire MW capability of battery is utilized, the revenue is high and so is the usage. In fact, the two quantities appear to be in direct proportion to the scaling factor in the average sense. It is also noteworthy that the spread increases as the scaling factor is increased. Another quantity worth analysis is the revenue per MWh used because it could be an estimate of the revenue from the battery over the battery's lifetime (measured in cycles). Fig. 7.4 shows the distribution revenue/usage for different scaling factors.

The significant difference in spread of the revenue plots in Fig. 7.3(a) is evened out to a certain extent in Fig. 7.4. Tables 7.1 and 7.2 tabulate the statistics from Figs. 7.3(a) and 7.4.

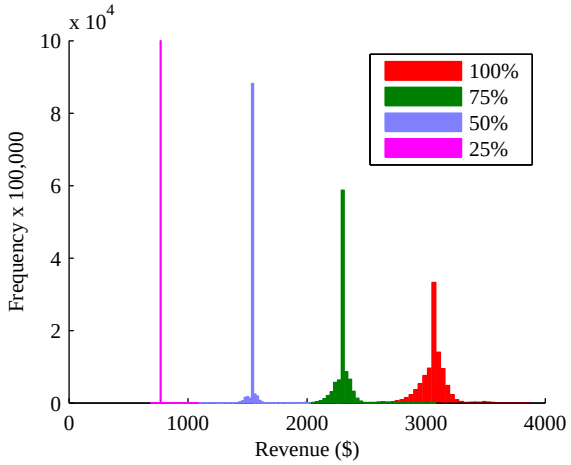

(a) Distribution of revenue for different values of the scaling factor.

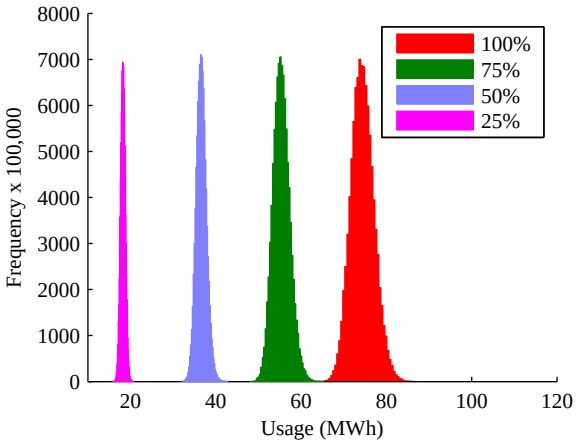

(b) Distribution of usage for different values of the scaling factor.

Figure 7.3: Results from Monte Carlo method

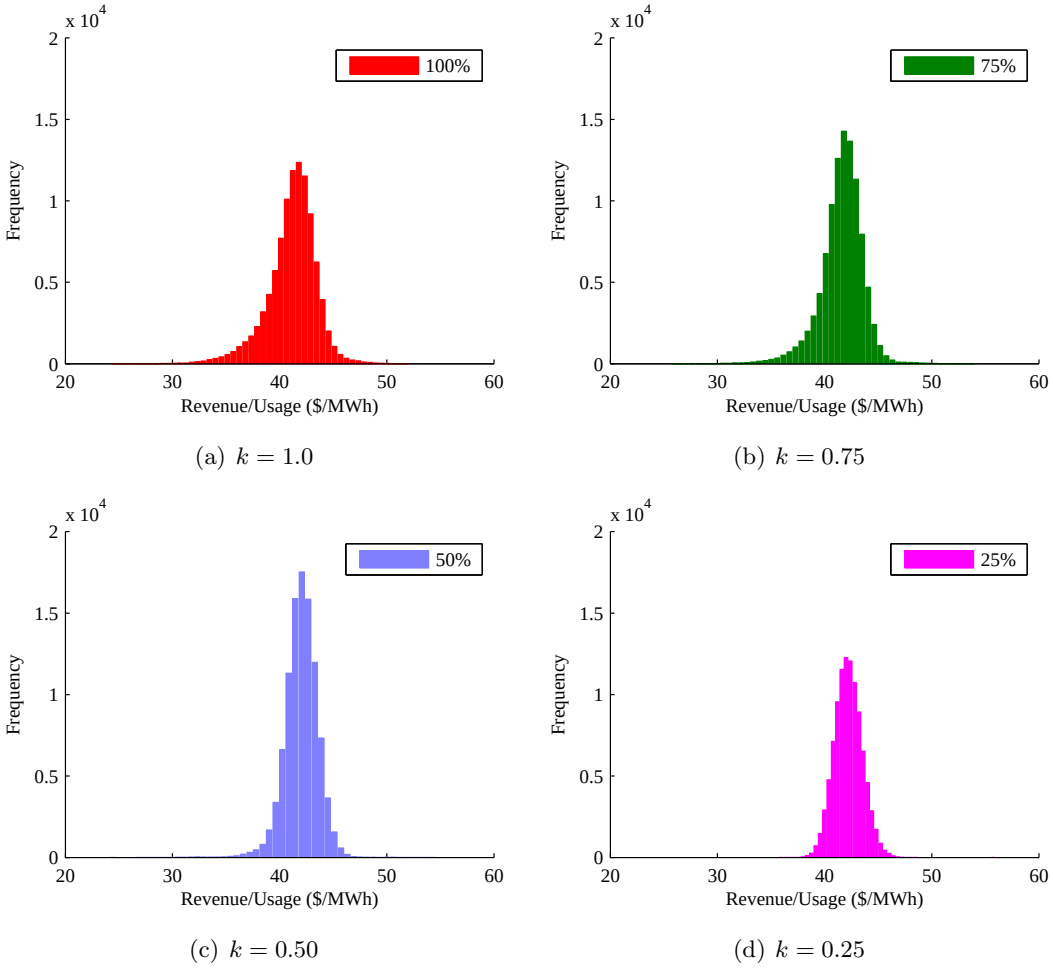

(a) $k = 1.0$ (b) $k = 0.75$

(c) $k = 0.50$ (d) $k = 0.25$

Figure 7.4: Distribution of revenue/usage for different values of the scaling factor.

Scaling	median ($)	mean($)	sd($)	95% C.I.
100%	3076.80	3057.70	121.75	2771.10 – 3257.30
75%	2307.60	2301.30	69.79	2148.60 – 2412.80
50%	1538.40	1537.60	26.26	1483.70 – 1577.40
25%	769.21	769.20	1.16	769.21 – 769.21

Table 7.1: Revenue statistics

Scaling	median ($/MWh)	mean($/MWh)	sd($/MWh)	95% C.I.
100%	41.4378	41.1619	2.27	35.6698 – 44.8891
75%	41.7776	41.5904	1.9766	36.8953 – 44.8290
50%	42.0764	42.0217	1.5716	38.8208 – 44.8199
25%	42.1742	42.2044	1.2985	39.7489 – 44.8258

Table 7.2: Revenue/usage statistics

Concluding remarks

As prefaced, this analysis considers a 1 MW, 7.2 MWh battery. If only 90% depth of discharge (DOD) is permitted, then a usage of $7.2 \times 2 \times 90/100$ equals 12.96 MWh. This usage also corresponds to one charge-discharge cycle. From Tables 7.1 and 7.2, the highest revenue scenario has a median revenue/usage of 41.4378 $/MWh. This will translate to a revenue of $537.03/cycle. The battery lifetime for 90% DOD is 4,500 cycles [32], meaning a lifetime revenue of $2,416,652.50 under the fastest return on investment scenario.

Chapter 8

Conclusion and Discussion

The ability of energy storage to shift generation effectively from off-peak to on-peak has been established by field results. Furthermore, the value added by shifting wind generation from off-peak to on-peak using energy storage has also been analyzed, and an optimal ratio of storage to wind has been suggested.

It is shown from the field results that the battery can effectively smooth the variations in wind generation, and simulation results totaling a simulated time of 30 years have been presented. It is also shown how wind smoothing can be integrated with wind generation shifting, enhancing the value added. The optimal storage to wind ratio for generation shifting was found to be highly effective for smoothing the wind generation as well.

The error from wind power forecast using Persistence method has been examined on a local and aggregated basis. It is shown that Normal distribution is a good approximation for the aggregated error but not for the local error. A statistical model for the local error has been developed and used to estimate the penalties for Uninstructed Deviations. The value of energy storage towards compensating for these deviations has been discussed.

A dispatch strategy, based on the extremeness of prices has been proposed for dispatching energy storage in the spot market. The parameters of the energy storage and the strategy have been optimized: it is shown that a higher energy capacity (MWh/MW) and conservative storage operation is most favorable from a financial standpoint.

Another economic dispatch strategy developed by Xcel Energy has been discussed

and used to find the best location to site the battery, again from a financial standpoint. It is understood that such a location would also be favorable from a transmission system point of view.

An analysis of the battery in the MISO operating reserve market has been presented, and possible revenue from the battery has been calculated.

The value from ramp rate limiting has not been calculated. Per the discussions with Xcel Energy, a consistent framework for assigning costs and value does not exist for this value proposition because of the diversity of the generation mix. Furthermore, it was found that the benefits from adding storage to compensate for forecast errors are minuscule, and not enough to justify the investment in storage. Moreover, it was strongly suggested by a reviewer during the review of [59], a publication from the research presented in chapter 4, that energy storage installed to compensate for forecast errors should be applied at the system level. Storage applied at the system level to compensate for forecast errors is essentially an operating reserve and the value as a reserve has been analyzed in chapter 7.

Table 8.1 lists the approximate value from the applications for which $ values have been calculated.

Application	Lifetime value
Generation shifting	$1,539,000[1]
Economic dispatch (chapter 5)	$1,549,000[2]
Economic dispatch (chapter 6)	$1,600,000[3]
Operating reserve	$2,417,000[4]

Table 8.1: $ values for select applications

All the analyses have slightly different assumptions/conditions. If these differences are ignored, it is seen from Table 8.1 that the returns are similar for generation shifting

[1] Calculated at Hub.

[2] Calculated at Hub. 100% efficiency assumed. The P/L ratio is expected to be higher for 7.2 MWh/MW

[3] Calculated at the best location. Parameters not optimized.

[4] Calculated using systemwide prices. 100% efficiency assumed.

and economic dispatch. Although the returns from energy trading component of generation shifting are low (Fig. 2.5), other components add further value, making generation shifting comparable to economic dispatch.

The returns from offering the battery as an operating reserve are significantly higher than other modes. This is because the battery could be earning revenue without charging/discharging at the cleared MWs, and thereby producing returns without incurring any loss in the lifetime.

However, with the exception of generation shifting, the rate of returns (in time) is never high enough to ensure the estimated returns within the calendar life of the battery. Therefore, multiple modes of operation should be integrated to further enhance the value and guarantee the estimated, or higher, return on the investment.

References

[1] EIA's Energy in Brief: How much renewable energy do we use? [Online]. Available: http://www.eia.gov/energy_in_brief/renewable_energy.cfm

[2] States with Renewable Portfolio Standards. The U.S. Department of Energy. [Online]. Available: http://apps1.eere.energy.gov/states/maps/renewable_portfolio_states.cfm

[3] "Directive 2001/77/EC of the European Parliament and the Council of 27 September 2001 on the Promotion of Electricity Produced From Renewable Energy Sources in the Internal Electricity Market."

[4] "20% Wind Energy by 2030," The U.S. Department of Energy, Tech. Rep. DOE/GO-102008-2567, July 2008. [Online]. Available: www.nrel.gov/docs/fy08osti/41869.pdf

[5] E. DeMeo, W. Grant, M. Milligan, and M. Schuerger, "Wind plant integration [wind power plants]," vol. 3, no. 6, pp. 38–46, Nov.-Dec. 2005.

[6] E. DeMeo, G. Jordan, C. Kalich, J. King, M. Milligan, C. Murley, B. Oakleaf, and M. Schuerger, "Accommodating wind's natural behavior," vol. 5, no. 6, pp. 59–67, Nov.-Dec. 2007.

[7] B. Parsons, M. Milligan, B. Zavadil, D. Brooks, B. Kirby, K. Dragoon, and J. Caldwell, "Grid impacts of wind power: A summary of recent studies in the United States," *Wind Energy*, vol. 7, no. 2, pp. 87–108, 2004.

[8] G. Dany, "Power reserve in interconnected systems with high wind power production," in *Power Tech Proceedings, 2001 IEEE Porto*, vol. 4, 2001, pp. 6 pp. vol.4–.

[9] R. Doherty and M. O'Malley, "A new approach to quantify reserve demand in systems with significant installed wind capacity," vol. 20, no. 2, pp. 587–595, May 2005.

[10] S. Watson, L. Landberg, and J. Halliday, "Application of wind speed forecasting to the integration of wind energy into a large scale power system," *Generation, Transmission and Distribution, IEE Proceedings-*, vol. 141, no. 4, pp. 357–362, Jul 1994.

[11] J. Casazza and F. Delea, *Understanding Electric Power Systems.* John Wiley & Sons, Inc., 2003.

[12] Henrik and Lund, "Large-scale integration of wind power into different energy systems," *Energy*, vol. 30, no. 13, pp. 2402 – 2412, 2005. [Online]. Available: http://www.sciencedirect.com/science/article/pii/S0360544204004736

[13] C. Wang and S. M. Shahidehpour, "Ramp-rate limits in unit commitment and economic dispatch incorporating rotor fatigue effect," *Power Systems, IEEE Transactions on*, vol. 9, no. 3, pp. 1539 – 1545, aug. 1994.

[14] G. Shrestha, K. Song, and L. Goel, "Strategic self-dispatch considering ramping costs in deregulated power markets," *Power Systems, IEEE Transactions on*, vol. 19, no. 3, pp. 1575 – 1581, aug. 2004.

[15] A. Nourai, V. Kogan, and C. Schafer, "Load leveling reduces T&D line losses," *Power Delivery, IEEE Transactions on*, vol. 23, no. 4, pp. 2168 –2173, oct. 2008.

[16] C. H. Lo and M. D. Anderson, "Economic dispatch and optimal sizing of battery energy storage systems in utility load-leveling operations," *Energy Conversion, IEEE Transactions on*, vol. 14, no. 3, pp. 824 –829, sep. 1999.

[17] B. Bhargava and G. Dishaw, "Application of an energy source power system stabilizer on the 10 MW battery energy storage system at Chino substation," *Power Systems, IEEE Transactions on*, vol. 13, no. 1, pp. 145 –151, feb. 1998.

[18] Midwest ISO. [Online]. Available: https://www.midwestiso.org/Pages/Home.aspx

[19] About NYISO - Understanding the Markets - The Energy Market. [Online]. Available: http://www.nyiso.com/public/about_nyiso/understanding_the_markets/energy_market/index.jsp

[20] PJM - Energy Market. [Online]. Available: http://pjm.com/markets-and-operations/energy.aspx

[21] European Transmission System Operators. [Online]. Available: http://www.etso-net.org/

[22] Australian Energy Market Operator (AEMO). [Online]. Available: http://www.aemo.com.au/

[23] Authority functions (Electricity Authority). [Online]. Available: http://www.ea.govt.nz/about-us/functions/

[24] "Wind power and electricity markets," Utility Wind Integration Group (UWIG), Tech. Rep., October 2011. [Online]. Available: http://www.uwig.org/windinmarketstableOct2011.pdf

[25] Y. V. Makarov, C. Loutan, J. Ma, and P. de Mello, "Operational impacts of wind generation on California power systems," vol. 24, no. 2, pp. 1039–1050, May 2009.

[26] C. Anderson and J. Cardell, "Reducing the variability of wind power generation for participation in day ahead electricity markets," in *Hawaii International Conference on System Sciences, Proceedings of the 41st Annual*, Jan. 2008, pp. 178–178.

[27] Energy and Operating Reserve Markets Business Practices Manual. Midwest ISO. [Online]. Available: https://www.midwestiso.org/Library/Pages/Library.aspx

[28] P. Ruiz and P. Sauer, "Spinning contingency reserve: Economic value and demand functions," *Power Systems, IEEE Transactions on*, vol. 23, no. 3, pp. 1071 –1078, aug. 2008.

[29] J. Wang, X. Wang, and Y. Wu, "Operating reserve model in the power market," *Power Systems, IEEE Transactions on*, vol. 20, no. 1, pp. 223 – 229, feb. 2005.

[30] J. Morales, A. Conejo, and J. Perez-Ruiz, "Simulating the impact of wind production on locational marginal prices," *Power Systems, IEEE Transactions on*, vol. 26, no. 2, pp. 820 –828, may 2011.

[31] (2008, Feb) Xcel Energy launches groundbreaking wind-to-battery project. [Online]. Available: http://www.xcelenergy.com/About_Us/Energy_News/News_Archive/Xcel_Energy_launches_groundbreaking_wind-to-battery_project

[32] "The NAS battery system for utility-scale energy storage (catalog)," NGK Insulators.

[33] B. L. Norris, J. Newmiller, and G. Peek, "NAS Battery Demonstration at American Electric Power," SAND2006-6740, Sandia National Labs (Albuquerque, NM, USA), Tech. Rep., March 2007.

[34] Market Settlements Business Practices Manual. Midwest ISO. [Online]. Available: https://www.midwestiso.org/Library/Pages/Library.aspx

[35] Production Tax Credit for Renewable Electricity Generation. U.S. Energy Information Administration. [Online]. Available: http://www.eia.gov/oiaf/aeo/otheranalysis/aeo_2005analysispapers/prcreg.html

[36] CPI Inflation Calculator. U.S. Department of Labor, Bureau of Labor Statistics. [Online]. Available: http://www.bls.gov/data/inflation_calculator.htm

[37] G. Giebel, R. Brownsword, and G. Kariniotakis, "The state-of-the-art in short-term prediction of wind power. A literature overview," Risø National Laboratory, Tech. Rep., 2003. [Online]. Available: http://anemos.cma.fr/download/ANEMOS_D1.1_StateOfTheArt_v1.1.pdf

[38] G. Kariniotakis, I.-P. Waldl, I. Marti, G. Giebel, T. Nielsen, J. Tambke, J. Usaola, F. Dierich, A. Bocquet, and S. Virlot, "Next generation forecasting tools for the optimal management of wind generation," in *Probabilistic Methods Applied to Power Systems, 2006. PMAPS 2006. International Conference on*, June 2006, pp. 1–6.

[39] T. Barbounis, J. Theocharis, M. Alexiadis, and P. Dokopoulos, "Long-term wind speed and power forecasting using local recurrent neural network models," vol. 21, no. 1, pp. 273–284, March 2006.

[40] U. Focken, M. Lange, K. Mnnich, H.-P. Waldl, H. G. Beyer, and A. Luig, "Short-term prediction of the aggregated power output of wind farms–a statistical analysis of the reduction of the prediction error by spatial smoothing effects," *Journal of Wind Engineering and Industrial Aerodynamics*, vol. 90, no. 3, pp. 231 – 246, 2002.

[41] T. Nielsen, A. Joensen, H. Madsen, L. Landberg, and G. Giebel, "A new reference for wind power forecasting," *Wind Energy*, vol. 1, no. 1, pp. 29–34, January 1998.

[42] L. Landberg, "Short-term prediction of the power production from wind farms," *Journal of Wind Engineering and Industrial Aerodynamics*, vol. 80, no. 1-2, pp. 207 – 220, 1999.

[43] M. Milligan, M. Schwartz, and Y. Wan, "Statistical wind power forecasting models: Results for U.S. wind farms," National Renewable Energy Laboratory, Tech. Rep. NREL/CP-500-33956, May 2003.

[44] A. Fabbri, T. GomezSanRoman, J. RivierAbbad, and V. MendezQuezada, "Assessment of the cost associated with wind generation prediction errors in a liberalized electricity market," vol. 20, no. 3, pp. 1440–1446, Aug. 2005.

[45] P. Pinson, C. Chevallier, and G. Kariniotakis, "Trading wind generation from short-term probabilistic forecasts of wind power," vol. 22, no. 3, pp. 1148–1156, Aug. 2007.

[46] H. Bludszuweit, J. Dominguez-Navarro, and A. Llombart, "Statistical analysis of wind power forecast error," vol. 23, no. 3, pp. 983–991, Aug. 2008.

[47] E. Farmer, V. Newman, and P. Ashmole, "Economic and operational implications of a complex of wind-driven generators on a power system," *Physical Science, Measurement and Instrumentation, Management and Education, Reviews, IEE Proceedings A*, vol. 127, no. 5, pp. 289–295, June 1980.

[48] Y. Zhang and K. W. Chan, "The impact of wind forecasting in power system reliability," in *Electric Utility Deregulation and Restructuring and Power Technologies, 2008. DRPT 2008. Third International Conference on*, April 2008, pp. 2781–2785.

[49] M. Black and G. Strbac, "Value of bulk energy storage for managing wind power fluctuations," vol. 22, no. 1, pp. 197–205, March 2007.

[50] L. Soder, "Reserve margin planning in a wind-hydro-thermal power system," vol. 8, no. 2, pp. 564–571, May 1993.

[51] A. Luig, S. Bofinger, and H. Beyer, "Analysis of confidence intervals for the prediction of regional wind power output," in *Proceedings of the European Wind Energy Conference, Copenhagen, Denmark*, 2001, pp. 2–6.

[52] S. Bofinger, A. Luig, and H. Beyer, "Qualification of wind power forecasts," in *Proceedings of Global Wind Power Conference*, April 2002.

[53] M. Ortega-Vazquez and D. Kirschen, "Estimating the spinning reserve requirements in systems with significant wind power generation penetration," vol. 24, no. 1, pp. 114–124, Feb. 2009.

[54] The Mathworks, Inc. [Online]. Available: http://mathworks.com/access/helpdesk/help/toolbox/stats/betafit.html

[55] C. W. Potter, D. Lew, J. McCaa, S. Cheng, S. Eichelberger, and E. Grimit, "Creating the dataset for the western wind and solar integration study (U.S.A.)," in *7th International Workshop on Large Scale Integration of Wind Power and on Transmission Networks for Offshore Wind Farms*, 2008. [Online]. Available: http://www.nrel.gov/wind/systemsintegration/pdfs/2008/lew_creating_dataset_wwsis.pdf

[56] NIST/SEMATECH e-handbook of statistical methods. [Online]. Available: http://www.itl.nist.gov/div898/handbook/

[57] D. S. Moore, G. P. McCabe, and B. A. Craig, *Introduction to the Practice of Statistics*, 6th ed. W. H. Freeman and Company, 2009.

[58] A. Akhil, S. Swaminathan, and R. Sen, "Cost analysis of energy storage systems for electric utility applications," SAND–97-0443, Sandia National Labs (Albuquerque, NM, USA), Tech. Rep., 1997.

[59] S. Tewari, C. Geyer, and N. Mohan, "A statistical model for wind power forecast error and its application to the estimation of penalties in liberalized markets," *Power Systems, IEEE Transactions on*, vol. 26, no. 4, pp. 2031 –2039, nov. 2011.

[60] Internal Revenue Bulletin - May 11, 2009 - Notice 2009-40. [Online]. Available: http://www.irs.gov/irb/2009-19_IRB/ar07.html

[61] M. H. DeGroot and M. J. Schervish, *Probability and Statistics*. Addison-Wesley, 2002.

[62] S. Tewari and N. Mohan, "Optimal strategy to dispatch storage in real-time markets," in *Summer Simulation Multiconference*, 2011.

Appendix A

Glossary and Acronyms

Some of the following definitions are in the context of Midwest ISO.

Ancillary Services	Under MISO, ancillary services are limited to operating reserves (see reserves).
Ancillary Services Market	A market in which reserves are sold to satisfy the reserve requirements designated by MISO.
ASM	Ancillary Services Market.
Capacity	MWs of firm (as opposed to intermittent) power that a generator can deliver.
Cut-in speed	The wind speed at which a wind turbine generator starts generating power.
Cut-out speed	The wind speed at which a wind turbine generator has to stop generating power because of safety considerations.
DA	Day Ahead, or Day Ahead market. A forward market for trading energy.

DALMP	The Locational Marginal Price of energy in the DA market at a given time and location.
Demand	The demand for electric energy. See load.
Demand response	An option towards managing electricity supply and demand by altering demand.
Dispatch	To dispatch a resource to meet demand.
DOD	Depth of discharge, complementary to the state of charge (SOC).
Energy storage	A technique or a device to store energy e.g. battery, flywheel.
Generation	Electric power generation.
baseload	Most rigid, but efficient generators designed to operate at their rated power for long intervals.
intermediate	Relatively flexible generators designed to follow the movements in demand.
peaking	Least efficient but very fast and flexible generators designed to serve peak demand.
ISO	Independent System Operator. An independent agency responsible for managing energy and ancillary services markets while promoting open access to transmission and fair competition.
LMP	Locational Marginal Price: the cost of meeting incremental demand at a given time and location.
Load	Consumer of electric energy, or the quantity of electrcity consumed.

Load leveling	The electric load varies throughout the day and the system is designed to reliably serve the peak load. Load leveling means making the load more uniform (less intra-day variability).
MCP	Market Clearing Price (of operating reserves under MISO).
MISO	Midwest Independent Transmission System Operator, Inc.
NSP	The region served by the former Northern States Power, now served by Xcel Energy.
Off-peak	The period when the load is not at its highest.
On-peak	The period when the load is at its highest.
Outage	Intentional or unintentional loss of generation.
PTC	Production tax credit. A credit for generating electricity from wind.
Ramp rate	The rate of change of generation (derivative).
Rated speed	The wind speed at which the wind farm starts generating its rated power.
Reserves	Generation available in excess of the generation required to meet peak load
regulating	Physically balance supply and demand in real time, maintain frequency.
spinning	Slower than regulating reserve, must provide energy in case of loss in generation.
standing	Same as spinning, but could be offline. Must be deployable within a small interval.

RT	Real Time, or Real Time market. A spot market for trading energy.
RTLMP	The Locational Marginal Price of energy in the RT market at a given time and location.
RTO	Regional Transmission Operator. See ISO
SCED	Security Constrained Economic Dispatch: dispatch committed resources at the lowest possible cost under reliability constraints.
SCUC	Security Constrained Unit Commitment: commit the resources to meet demand reliably.
SOC	The energy left in the battery, normalized against the maximum possible energy stored.
Transmission	The high voltage network of lines to transfer power from generation to load.
TSO	Transmission system operator. See ISO.
Uninstructed Deviation	Deviation from the dispatch instruction sent by the ISO.
VOLL	Value of lost load. The maximum price a load would pay to prevent interruption in electricity supply.